Foundation for Cancer Research, for helpful advice with the statistical analyses.

REFERENCES

1. Cooper WA, Thourani VH, Gal AA, et al. The surgical spectrum of pulmonary neurocrine neoplasms. *Chest* 2001;119:14–18.
2. Garcia-Yuste M, Matilla JM, Alvarez-Gago T, et al. Prognostic factors in neuroendocrine lung tumors: a Spanish multicenter study. *Ann Thorac Surg* 2000;70:258–263.
3. Jones MH, Virtanen C, Honjoh D, et al. Two prognostically significant subtypes of high-grade lung neuroendocrine tumors independent of small-cell and large-cell neuroendocrine carcinomas identified by gene expression profiles. *Lancet* 2004;363:775–781.
4. Travis WD, Linnoila RI, Tsokos MG, et al. Neuroendocrine tumors of the lung with proposed criteria for large cell neuroendocrine carcinoma. An ultrastructural, immunohistochemical, and flow cytometric study of 35 cases. *Am J Surg Pathol* 1991;15:529–533.
5. Asamura H, Kameya T, Matsuno Y, et al. Neuroendocrine neoplasms of the lung: a prognostic spectrum. *J Clin Oncol* 2006;24:70–76.
6. Dresler CM, Ritter JH, Patterson GA, et al. Clinical-pathologic analysis of 40 patients with large cell neuroendocrine carcinoma of the lung. *Ann Thorac Surg* 1997;63:180–185.
7. Fernandez FG, Battafarano RJ. Large cell neuroendocrine carcinoma of the lung. *Cancer Control* 2006;13:270–275.
8. Hiroshima K, Iyoda A, Shida T, et al. Distinction of pulmonary large cell neuroendocrine carcinoma from small cell lung carcinoma: a morphological, immunohistochemical, and molecular analysis. *Mod Pathol* 2006;19:1358–1368.
9. Iyoda A, Hiroshima K, Nakatani Y, et al. Pulmonary large cell neuroendocrine carcinoma: its place in the spectrum of pulmonary carcinoma. *Ann Thorac Surg* 2007;84:702–707.
10. Iyoda A, Hiroshima K, Toyozaki T, et al. Adjuvant chemotherapy for large cell carcinoma with neuroendocrine features. *Cancer* 2001;92:1108–1112.
11. Jiang SX, Kameya T, Shoji M, et al. Large cell neuroendocrine carcinoma of the lung: a histologic and immunohistochemical study of 22 cases. *Am J Surg Pathol* 1998;22:526–537.
12. Travis WD, Gal AA, Colby TV, et al. Reproducibility of neuroendocrine lung tumor classification. *Hum Pathol* 1998;29:272–279.
13. Wick MR, Berg LC, Herts MI. Large cell carcinoma of the lung with neuroendocrine differentiation: a comparison with large cell "undifferentiated" pulmonary tumors. *Am J Surg Pathol* 1992;97:796–805.
14. Veronesi G, Morandi U, Alloisio M, et al. Large cell neuroendocrine carcinoma of the lung: a retrospective analysis of 144 surgical cases. *Lung Cancer* 2006;53:111–115.
15. Travis WD, Colby TV, Corrin B, et al. *Histological Typing of Lung and Pleural Tumors. 3rd Ed. World Health Organization International Histological Classification of Tumors.* Berlin: Springer Verlag, 1999.
16. Colby TV, Koss MN, Travis WD. *Tumors of the Lower Respiratory Tract. Atlas of Tumor Pathology.* 3rd series. Washington DC: Armed Forces Institute of Pathology, 1995:248–255.
17. Hiroshima K, Abe S, Ebihara Y, et al. Cytological characteristics of pulmonary large cell neuroendocrine carcinoma. *Lung Cancer* 2005;48:331–337.
18. Iyoda A, Baba M, Hiroshima K, et al. Imprint cytologic features of pulmonary large cell neuroendocrine carcinoma: comparison with classic large cell carcinoma. *Oncol Rep* 2004;11:285–288.
19. Jimenez-Heffernan JA, Lopez-Ferrer P, Vicandi B, et al. Fine-needle aspiration cytology of large cell neuroendocrine carcinoma of the lung: a cytopathologic correlation study of 11 cases. *Cancer* 2008;114:180–186.
20. Kakinuma H, Mikami T, Iwabuchi K, et al. Diagnostic findings of bronchial brush cytology for pulmonary large cell neuroendocrine carcinomas. *Cancer (Cancer Cytopathol)* 2003;99:247–254.
21. Nicholson SA, Ryan MR. A review of cytologic findings in neuroendocrine carcinomas including carcinoid tumor with histologic correlation. *Cancer (Cancer Cytopathol)* 2000;90:148–161.
22. Wiatrowska BA, Krol J, Zakowski MF. Large cell neuroendocrine carcinoma of the lung: proposed criteria for cytologic diagnosis. *Diagn Cytopathol* 2001;24:58–64.
23. Nicholson SA, Beasley MB, Brambilla E, et al. Small cell lung carcinoma (SCLC): a clinicopathologic study of 100 cases with surgical specimens. *Am J Surg Pathol* 2002;26:1184–1197.

Tumorigenesis and Neoplastic Progression

Function of *EWS-POU5F1* in Sarcomagenesis and Tumor Cell Maintenance

Takashi Fujino,[*†] Kimie Nomura,[‡]
Yuichi Ishikawa,[‡] Hatsune Makino,[§]
Akihiro Umezawa,[§] Hiroyuki Aburatani,[¶]
Koichi Nagasaki,[‖] and Takuro Nakamura[*]

From the Divisions of Carcinogenesis,[*] and Pathology,[‡] and the Genome Center,[‖] The Cancer Institute, Japanese Foundation for Cancer Research, Tokyo; the Department of Pathology,[†] Faculty of Medicine, Kyorin University, Tokyo; the Department of Reproductive Biology,[§] National Institute for Child and Health Development, Tokyo; and the Genome Research Division,[¶] Research Center for Advanced Science and Technology, University of Tokyo, Tokyo, Japan

POU5F1 is a transcription factor essential for the self-renewal activity and pluripotency of embryonic stem cells and germ cells. We have previously reported that *POU5F1* is fused to *EWSR1* in a case of undifferentiated sarcoma with chromosomal translocation t(6;22)(p21;q12). In addition, the *EWS-POU5F1* chimeras have been recently identified in human neoplasms of the skin and salivary glands. To clarify the roles of the *EWS-POU5F1* chimera in tumorigenesis and tumor cell maintenance, we used small-interfering RNA-mediated gene silencing. Knockdown of *EWS-POU5F1* in the t(6;22) sarcoma-derived GBS6 cell line resulted in a significant decrease of cell proliferation because of G1 cell cycle arrest associated with p27[Kip1] up-regulation. Moreover, senescence-like morphological changes accompanied by actin polymerization were observed. In contrast, *EWS-POU5F1* down-regulation markedly increased the cell migration and invasion as well as activation of metalloproteinase 2 and metalloproteinase 14. The results indicate that the proliferative activity of cancer cells and cell motility are discrete processes in multistep carcinogenesis. These findings reveal the functional role of the sarcoma-related chimeric protein as well as POU5F1 in the development and progression of human neoplasms. *(Am J Pathol 2010, 176:1973–1982; DOI: 10.2353/ajpath.2010.090486)*

POU5F1/OCT4 is an essential transcription factor for the formation and/or maintenance of the inner cell mass of the mammalian blastocyst, the origin of pluripotent em-

bryonic stem (ES) cells.[1–3] Suppression of *POU5F1* expression converts ES cells to trophoblasts, whereas overexpression of *POU5F1* leads to differentiation toward endoderm and mesoderm.[3,4] The self-renewal activity and pluripotency of ES cells are suppressed by knockdown of *POU5F1*.[5] These data suggest that POU5F1 orchestrates target gene expression in a tightly regulated manner during development and cellular differentiation. Also, POU5F1 induces reprogramming of somatic cells into iPS cells in combination with Sox2, c-Myc, and Klf4.[6] Moreover, two factors, either POU5F1 and Klf4 or POU5F1 and c-Myc, are apparently sufficient to generate iPS cells.[7]

In carcinogenesis, up-regulated expression of *POU5F1* is significantly correlated to certain lineages of human malignancies including germ cell tumors and breast and bladder cancer.[8–11] Reactivation of POU5F1 in somatic cells may induce dedifferentiation and may disrupt homeostasis, resulting in malignant transformation. Direct involvement of POU5F1 has been detected in a case of undifferentiated bone sarcoma with t(6;22)(p21;q12) translocation in which *POU5F1* is fused to *EWSR1*.[12] The chimeric *EWS-POU5F1* protein is composed of a transactivation domain of EWS and the entire DNA-binding domain of POU5F1. Ectopic overexpression of the POU5F1 component is achieved by the strong promoter activity of *EWSR1*.[12] Similar gene fusions between *EWSR1* and *POU5F1* have been identified in hidradenoma of the skin and mucoepidermoid carcinoma of the salivary glands.[13] These results underscore the important role of dysregulated *POU5F1* expression in human cancer and the important contributions of *EWS-POU5F1* to the development and maintenance of cancer cells.

In this study, we knocked down *EWS-POU5F1* by using *POU5F1*-specific small-interfering RNAs (siRNAs) in

1973

the GBS6 cell line established from the t(6;22) undifferentiated sarcoma.[12] Cellular growth was significantly suppressed by *EWS-POU5F1* depletion and was accompanied by up-regulation of p27^{Kip1} expression, and senescence-like morphological alterations were observed. On the other hand, cell motility and invasive capacity were dramatically increased, and promotion of actin polymerization and activation of metalloproteinase (MMP)14 and MMP2 were observed. These results suggest that EWS-POU5F1 promotes proliferation of cancer cells but is dispensable for or even inhibits cell motility and invasiveness. This study provides important insights into EWS-POU5F1 function in carcinogenesis and tumor cell maintenance.

Materials and Methods

Cell Culture

The GBS6 cell line was established from a pelvic bone undifferentiated sarcoma with t(6;22)(p21;q12).[12] The cells were maintained at 37°C under 5% CO_2 in RPMI 1640 medium supplemented with 10% fetal bovine serum and 10 mmol/L of HEPES buffer, pH7.4. NIH3T3, HeLa, and HCT116 cells were grown at 37°C under 5% CO_2 in Dulbecco's modified Eagle's medium supplemented with 10% fetal bovine serum.

RNA Interference and DNA Transfection

RNA interference and DNA transfection experiments were performed by using Lipofectamine 2000 (Invitrogen, Carlsbad, CA). GBS6 cells were seeded on 12-well plates 24 hours before transfection at a density of 1 × 10⁵ or 2.5 × 10⁵ cells per well for siRNAs or plasmid DNAs, respectively. GBS6 cells were then transfected with 60 pmol or 1.6 μg of siRNAs or plasmids, respectively. The following siRNAs were purchased from Qiagen (Hilden, Germany): siRNA-POU5F1-1 (SI00690389) and siRNA-POU5F1-2 (SI026617) and control (non-sil). A FLAG-tagged p27 expression plasmid was a kind gift from Dr. Kei-ichi Nakayama.

Senescence-Associated β-galactosidase Assay

Senescence-associated β-galactosidase was detected histochemically by using a Senescence Detection Kit (Biovision, Mountain View, CA) 4 days after transfection of siRNAs.

Western Blotting

Whole cell lysates were size-fractionated by SDS-polyacrylamide gel electrophoresis and were transferred onto a nitrocellulose membrane. The membrane was blocked with Tris-buffered saline (pH 7.5) containing 0.2% Tween 20 and 5% nonfat dry milk. Primary antibodies used were as follows: goat anti-Oct3/4 (1:500 dilution; C-20, Santa Cruz Biotechnology, Santa Cruz, CA), mouse anti-lamin A/C (1:500 dilution; Santa Cruz Biotechnology), rabbit anti-p27 (1:200 dilution; Santa Cruz Biotechnology), mouse anti-p53 (1:200 dilution; DO-1, Santa Cruz Biotechnology), mouse anti-p21 (1:100 dilution; BD Biosciences, San Diego, CA), mouse anti-Rb (1:500 dilution; IF8, Santa Cruz Biotechnology), rabbit anti-Phospho-Rb (Ser807/811; 1:500 dilution; Cell Signaling Technology, Beverly, MA), mouse anti-cyclin D1 (1:500 dilution; A-12, Santa Cruz Biotechnology), rabbit anti-CDK2 (1:500 dilution; M2, Santa Cruz Biotechnology), rabbit anti-CDK4 (1:500 dilution; H-22, Santa Cruz Biotechnology), rabbit anti-CDK6 (1:500 dilution; C-21, Santa Cruz Biotechnology), mouse anti-MMP14 (1:200 dilution; Daiichi Fine Chemical, Tokyo, Japan), and mouse anti-RhoA (1:200 dilution; Upstate Biotechnology, Temecula, CA). The signals were detected by using appropriate secondary antibodies and an enhanced chemiluminescence kit (GE Health care, Piscataway, NJ).

Flow Cytometric Analysis

Single cell suspensions were permeabilized with 0.1% triton X-100 in PBS, and 50 mg/ml of propidium iodide and 1 mg/ml of RNase A were added. The cell suspensions were then analyzed by using a FACS-calibur flow cytometer (Beckton Dickinson, Franklin Lakes, NJ) and Modfit software (Beckton Dickinson).

Cell Invasion and Migration Assays

A quantitative invasion assay was performed by using a BD BioCoat Matrigel invasion chamber with 8-μm pore size membranes (BD Biosciences) according to the manufacturer's instruction. Briefly, cells incubated with siRNAs or plasmid DNAs for 24 hours were trypsinized and resuspended at a density of 1 × 10⁵ cells per 1 ml of RPMI without serum. Cells (5 × 10⁵) were then loaded onto inserts of the upper chambers. RPMI with 10% fetal bovine serum was added to the lower chambers. After 24 hours of incubation, cells on the upper surface membranes were removed gently with a cotton swab. Cells on the lower surface were stained with Wright-Giemsa solutions and air-dried. Cell migration was also evaluated by using the same chambers without Matrigel by assessing the cell numbers within the lower chamber. The invading or migrating cells were counted, and images were obtained by using an Olympus BX41 microscope with a 20× objective (Olympus, Tokyo, Japan). For the wound healing assay, GBS6 cells were cultured for 48 hours after transfection of siRNAs to reach 90% confluence in 12-well plates. A linear scratch, 100 μm in width, was produced by using a plastic tip. Cells were incubated in growth medium for the indicated period. Images were photographed by using an Olympus IX70 phase contrast microscope. The distance of cell migration from the scratch line was measured in micrometers on the photographs.

Gelatin Zymography

Conditioned media from GBS6 cell cultures were harvested 48 hours after siRNA transfection, loaded on 10% gelatin gels (Invitrogen), and electrophoresed. The gels were stained with 0.25% Coomassie Blue and were destained in 5% acetic acid/10% methanol to visualize bands corresponding to the gelatinolytic activity.

Total RNA Extraction, Conventional RT-PCR, and Real-Time Quantitative RT-PCR

Total RNA extraction, reverse transcription, and RNA quantification were performed according to methods described previously.[14] Conventional RT-PCR was performed by using a Gene Amp 9700 thermal cycler (Applied Biosystems, Foster City, CA). We conducted 40 cycles of three-step PCR (95°C for 30 seconds, 55°C for 1 minute, and 72°C for 1 minute) for miR032-367 locus and 25 cycles of three-step PCR (95°C for 30 seconds, 60°C for 30 seconds, and 72°C for 30 seconds) for actin. The specific forward and reverse primers for optimal amplification were designed as follows: miR302-367 locus, 5'-GGGCTCCCTTCAACTTTAAC-3' and 5'-ATTCTGTCATTGGCTTAACAATCCATCACC-3'; β-actin, 5'-AGGCATCCTCACCCTGAAGTACCC-3' and 5'-GCCAGGTCCAGACGCAGG-3'. Real-time RT-PCR was performed by using a 7500 Fast Real-Time PCR System (Applied Biosystems) using the following parameters: 40 cycles of three-step PCR (95°C for 15 seconds, 60°C for 30 seconds, and 72°C for 30 seconds). The specific forward and reverse primers to produce approximately 60-bp amplicons for optimal amplification in real-time PCR were designed as follows: MMP2, 5'-CCGCAGTGACGGAAA-GATGT-3' and 5'-GCCCCACTTGCGGTCAT-3'; MMP14, 5'-CGAGAGGAAGGATGGCAAATT-3' and 5'-AGGGA-CGCCTCATCAAACAC-3'; β-actin, 5'-TGGATCAGCAAG-CAGGAGTATG-3' and 5'-GCATTTGCGGTGGACGAT-3'; and miR302-367 locus, 5'-TTTGAGTGTGGTGGTTCC-TACCT-3' and 5'- AGCCAAGAACTGCACACAGTGT-3'.

Actin Staining

GBS6 cells were seeded onto four-chamber culture slides (BD Biosciences) at a density of 3000 cells per well 24 hours after transfection and were incubated for an additional 24 hours in growth medium. Cells were then fixed and stained with phalloidin-rhodamine (Invitrogen). Images were photographed by using a Leica DM6000B laser scanning microscope with a 40× objective (Leica Microsystems, Cambridge, UK).

RhoA Activity Assay

To confirm RhoA activation, the amount of RhoA-GTP bound to the Rhotekin Rho-binding domain (RBD) was determined by using the Rho Activation Assay Kit (Upstate Biotechnology). Forty-eight hours after transfection of siRNAs, whole cell lysates were incubated with Rhotekin RBD-agarose for 45 minutes at 4°C. After washing, agarose beads were resuspended in Laemmli sample buffer, boiled for 5 minutes, and subjected to immunoblotting with an anti-RhoA antibody.

Microarray

The oligonucleotide array Human Genome U133 Plus 2.0 (Affymetrix, Santa Clara, CA), composed of 38,500 human genes and expressed sequence tags, was hybridized with cRNA probes generated from GBS6 cells 4 days after siRNA transfection and was scanned according to the method previously described.[14] The data were deposited in a public database (*http://www.ncbi.nlm.nih. gov/geo*, accession number: GSE12320, last accessed November 5, 2009). Clustering analysis was performed by using dChip software (*http://biosun1.harvard.edu/complab/ dchip/* last accessed October 14, 2009). The gene network was analyzed by Webgestalat (*http://bioinfo.vanderbilt. edu/webgestalt/* last accessed October 31, 2009).

Statistical Analysis

Results were evaluated statistically by using Student's t-test. A value of $P < 0.05$ was considered significant.

Results

EWS-POU5F1 *Knockdown Induces p27^{Kip1} Up-Regulation and G1 Arrest*

The GBS6 cell line was established from a t(6;22) undifferentiated sarcoma that expressed the chimeric *EWS-POU5F1* but not wild-type *POU5F1*.[12] To investigate the biological role of *EWS-POU5F1*, we knocked down *EWS-POU5F1* in GBS6 cells by RNA interference. Effective knockdown of *EWS-POU5F1* on 2 days after transfection was confirmed for two independent *POU5F1*-specific siRNAs (Figure 1A, 88.3% of reduction by siRNA-1 and 85.9% by siRNA-2). The effects of the two siRNAs were similar to each other in every experiment, and the results using siRNA-POU5F1-1 are exhibited subsequently as a representative.

Suppression of *EWS-POU5F1* in GBS6 cells was significantly inhibited proliferation, the cell numbers being 58% or 54% of those treated with a control siRNA on day 2 or day 4, respectively (Figure 1B). A terminal deoxynucleotidyl transferase-mediated dUTP nick-end labeling assay did not show an apparent increase of apoptotic cells during treatment with RNA interference (data not shown). This result suggests that the suppression of cell growth might be because of inhibition of the cell cycle. Flow cytometric analysis demonstrated that knockdown of *EWS-POU5F1* significantly decreased the S-phase population and increased the G1 fraction compared with the control (Figure 1C), indicating that cell growth of GBS6 was suppressed because of G1 arrest.

We next examined the expression of a series of cell cycle regulators. Increased expression of p27 was observed in GBS6 cells during *EWS-POU5F1* knockdown (Figure 1D, left). An RT-PCR experiment showed no significant decrease of *p27* mRNA during *EWS-POU5F1*
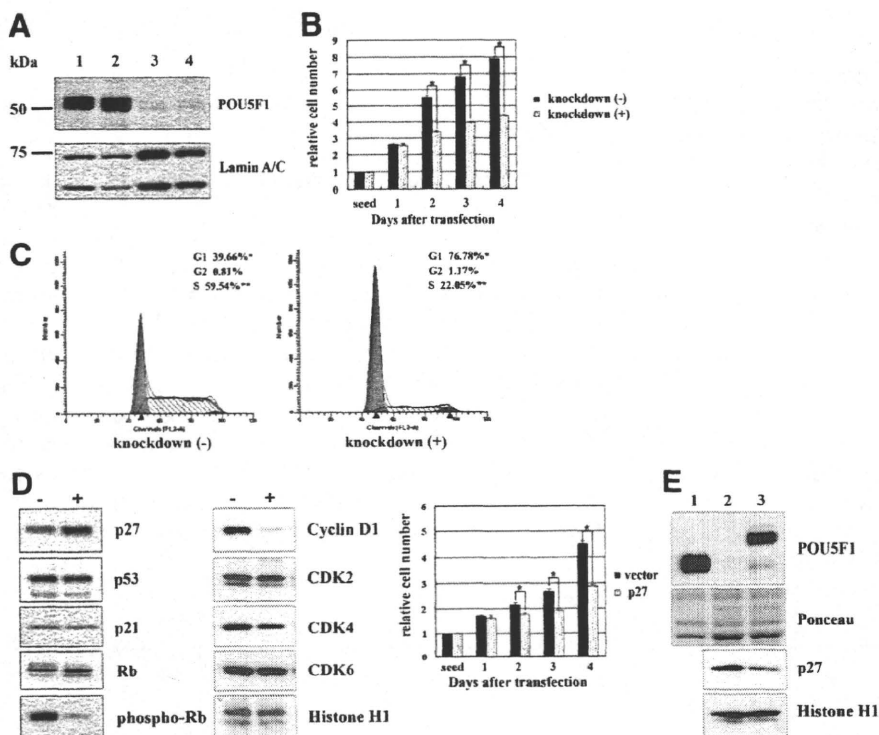
Figure 1. Knockdown of *EWS-POU5F1* inhibits proliferation of GBS6 cells accompanied by G1 cell cycle arrest and up-regulation of p27. **A:** RNA interference. GBS6 cells were transfected with control or *POU5F1* siRNAs and harvested 2 days after transfection; lysates were subjected to Western blotting by using anti-POU5F1 antibody. Lamin A/C was used as a control. **Lane 1**, wild-type; **lane 2**, negative control siRNA (non-sil); **lane 3**, POU5F1 siRNA-1; **lane 4**, POU5F1 siRNA-2. **B:** Proliferation assay of GBS6 cells treated with non-sil or POU5F1 siRNA. Mean of relative cell numbers ± SE of three independent experiments are presented (*$P < 0.005$). **C:** Flow cytometric analysis of GBS6 cells treated with siRNAs. Average percentages of G1, G2, and S phases in three experiments are indicated. *$P < 0.005$. **D:** Western blotting of GBS6 cells transfected with control (−) or POU5F1 (+) siRNAs by using antibodies specific for the indicated protein. Histone H1 was used as a loading control (**left**); proliferation assay (**right**) of GBS6 cells in which p27 was introduced. Mean of relative cell numbers ± SE of three independent experiments are presented (*, **$P < 0.005$). **E:** Western blotting of GBS6 cells and NIH3T3 cells transfected with an empty or *EWS-POU5F1* vectors by using anti-POU5F1 or anti-p27. **Lane 1**, GBS6 cells; **lane 2**, NIH3T3 treated with an empty vector; and **lane 3**, NIH3T3 treated with an *EWS-POU5F1* expression vector. Ponceau staining and Histone H1 were used as a loading control.

suppression (data not shown), suggesting that the change might be indirect and *p27* was not transcriptionally regulated by EWS-POU5F1. During knockdown, phosphorylation of Rb protein on Ser807/811 was significantly decreased, whereas expression of total Rb protein remained unchanged (Figure 1D, left). Expression of p21 and p53 was not affected (Figure 1D, left). In addition, a comparative genomic hybridization analysis revealed a homozygous loss of *p16^INK4A^/p14^ARF^* (Supplemental Figure S1, see *http://ajp.amjpathol.org*). A significant decrease of cyclin D1 expression was also noted (Figure 1D, left). On the other hand, expression of CDK2, CDK4, and CDK6 was unchanged (Figure 1D, left).

Exogenous introduction of *p27* into GBS6 cells resulted in 82% and 61% decreased proliferation compared with the transfected controls on days 2 and 4, respectively (Figure 1D, right). Conversely, exogenous expression of *EWS-POU5F1* in NIH3T3 cells markedly depleted p27 (Figure 1E). However, expression of *EWS-POU5F1* did not affect proliferation of NIH3T3 cells, suggesting that the effect might be cell context-dependent. Taken together, these results indicate that EWS-POU5F1 supports tumor cell growth, at least in part, through down-regulating the p27[Kip1] activity.

Induction of the Senescence-Like Morphology by EWS-POU5F1 Knockdown

GBS6 cells possess a short spindle-shaped morphology with a narrow cytoplasm and a small nucleus with rough heterochromatin (Figure 2A, left), reflecting the original phenotype *in vivo*.[12] After introduction of *POU5F1*-specific siRNAs, we observed prompt enlargement of GBS6 cell bodies. Most GBS6 cells demonstrated large and flat cyto-

plasms as well as enlarged nuclei with fine chromatins 4 days after siRNA transfection. This morphology mimicked that observed in cellular senescence (Figure 2A, right). Most of the GBS6 cells enlarged by *EWS-POU5F1* knockdown expressed senescence-associated β-galactosidase (Figure 2B), a well-established biomarker of senescence.[15] However, senescence-associated heterochromatin foci, another biomarker of senescence,[16] were not observed (data not shown). Importantly, the enlarged GBS6 phenotype (and growth arrest) mediated by *POU5F1*-specific siRNAs disappeared 10 days after transfection when *EWS-POU5F1* expression returned (data not shown). Thus, the change was transient and reversible. These data suggest that the phenotypic changes were not because of senescence but rather indicated G1 arrest. Interestingly, overexpression of *p27^Kip1^* did not induce morphological changes in GBS6 cells (data not shown), indicating that different molecular pathways downstream of EWS-POU5F1 are responsible for the senescence-like morphologies.

Drastic modification of the cytoskeleton was also observed in siRNA-treated enlarged GBS6 cells. Phalloidin staining revealed prominent networks of F-actin throughout the cytoplasm of siRNA-treated cells (Figure 2C, right). Control GBS6 cells showed only a small amount of actin fibers in the cytoplasmic rim (Figure 2C, left). A close link between actin polymerization and a small G protein Rho has been reported.[17] Indeed, a GTP-bound activated form of RhoA protein was apparently increased on *EWS-POU5F1* knockdown (Figure 2D). These data indicate that EWS-POU5F1 affected the RhoA signaling pathway and morphology of tumor cells by modulating the actin fiber network. Finally, transfection of *POU5F1*-specific siRNA into HeLa cells that do not express *POU5F1* did not affect cell morphology (Figure 2E), indi-
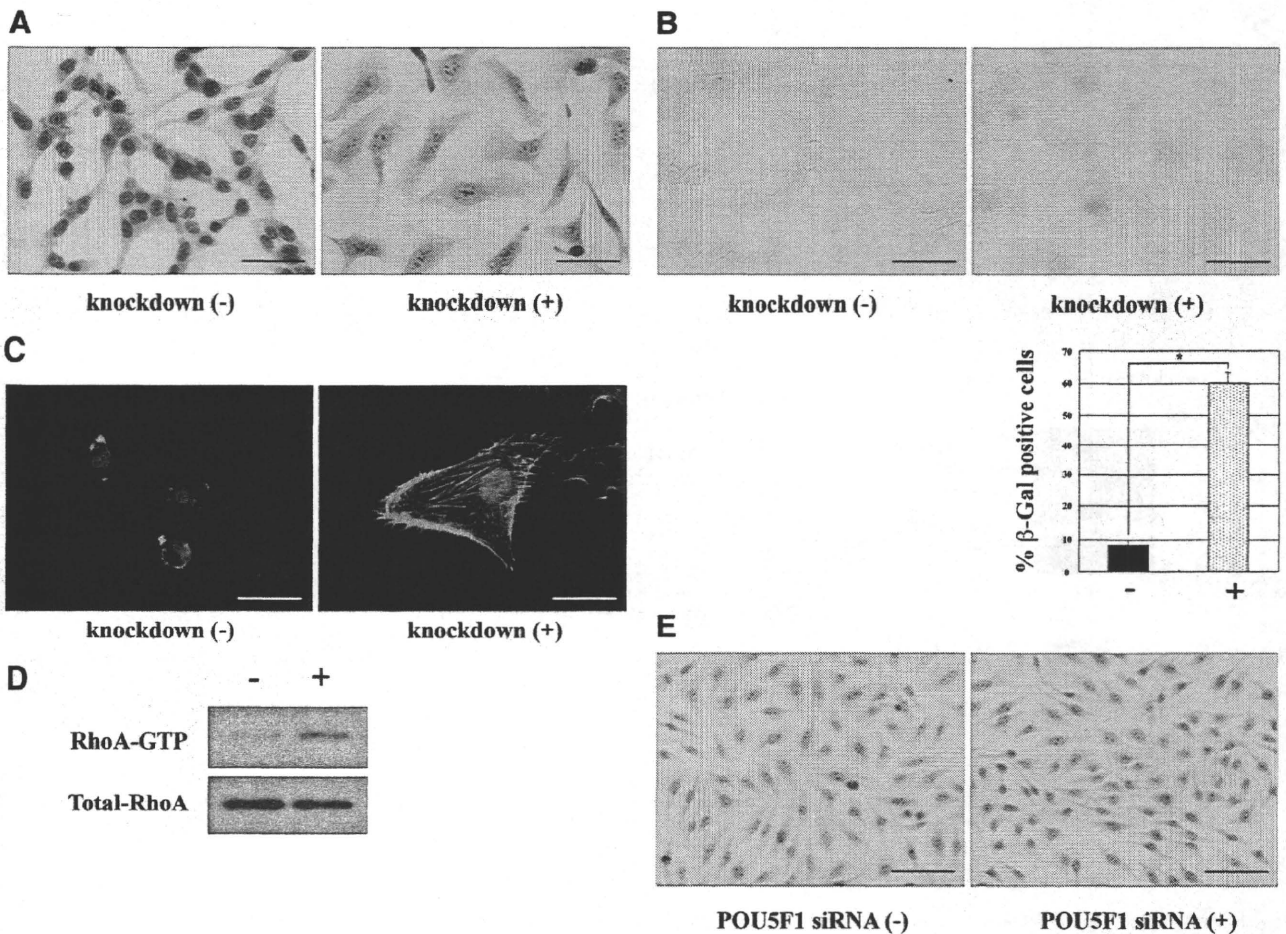
A

knockdown (-)   knockdown (+)

B

knockdown (-)   knockdown (+)

C

knockdown (-)   knockdown (+)

D   -   +

RhoA-GTP

Total-RhoA

E

POU5F1 siRNA (-)   POU5F1 siRNA (+)

Figure 2. Morphological changes and actin polymerization in siRNA-treated GBS6 cells. **A:** Photomicrographs of GBS6 cells transfected with control siRNA or *POU5F1*-specific siRNA. Papanicolau staining, ×400 original magnification. Scale bars = 100 μm. **B:** Senescence-associated β-galactosidase (SA-β-Gal) assay 4 days after transfection of siRNAs. Original magnification, ×400. Scale bars = 100 μm. The columns indicate mean % SA-β-Gal-positive cells in three independent experiments ($*P < 0.005$). **C:** Enhanced actin polymerization in *EWS-POU5F1* silent GBS6 cells. F-actin was visualized by phalloidin-rhodamine staining. Original magnification, ×400. Scale bars = 100 μm. **D:** Increased RhoA-GTP in *EWS-POU5F1* silenced GBS6 cells (+) compared with control (−). **E:** *POU5F1* knockdown does not affect morphology of HeLa cells. Papanicolau staining, ×200 original magnification. Scale bars = 100 μm.

cating that the above findings are not because of non-specific effects of *POU5F1* siRNAs.

Knockdown of EWS-POU5F1 *Promotes Cell Migration and Invasion*

Uncontrolled proliferation and metastatic activities are important biological characteristics of cancer.[18] Indeed, in the t(6;22) sarcoma case, the patient died of multiple pulmonary metastases.[12] Therefore, it is intriguing to clarify whether EWS-POU5F1 promotes cell migration and invasiveness. Migration and invasion of GBS6 cells treated with siRNA for *EWS-POU5F1* were assessed in a Matrigel invasion assay. *EWS-POU5F1* knockdown resulted in marked increases in migration and invasion activities compared with the control GBS6 cells (Figure 3A and Table 1). The original GBS6 cells rarely migrated *in vitro*; however, the number of cells migrating in the absence of EWS-POU5F1 increased more than 50-fold. The increase in cell motility after *EWS-POU5F1* knockdown was also confirmed by a wound healing assay, showing that GBS6 cells with *EWS-POU5F1*

knockdown migrated 2.5-fold faster than the control cells (Figure 3B).

We next asked whether the enhanced invasiveness of GBS6 cells in Matrigel was solely because of increased cell motility or whether invasiveness itself was also accelerated. Because cell invasion activity is closely associated with increased metalloproteinase activity,[19,20] MMP2 and MMP9 activities were assessed by gelatin zymography. The zymogram exhibited a significant increase of the gelatinolytic activity of MMP2, whereas the MMP9 activity was not altered (Figure 3C, top). MMP14/MT1-MMP, a membrane-type MMP, activates pro-MMP2 in collaboration with a tissue inhibitor of metalloproteinase 2.[19,21] An immunoblot analysis demonstrated increased expression of the MMP14 protein (Figure 3C, bottom), consistent with promotion of MMP2 activity. Thus, *EWS-POU5F1* knockdown increased cell motility and also enhanced invasiveness through accelerated degradation of matrix by MMPs.

Real-time quantitative RT-PCR showed that expression of MMP2 and MMP14 was also increased at the RNA level (Figure 3D), suggesting that *EWS-POU5F1* may also
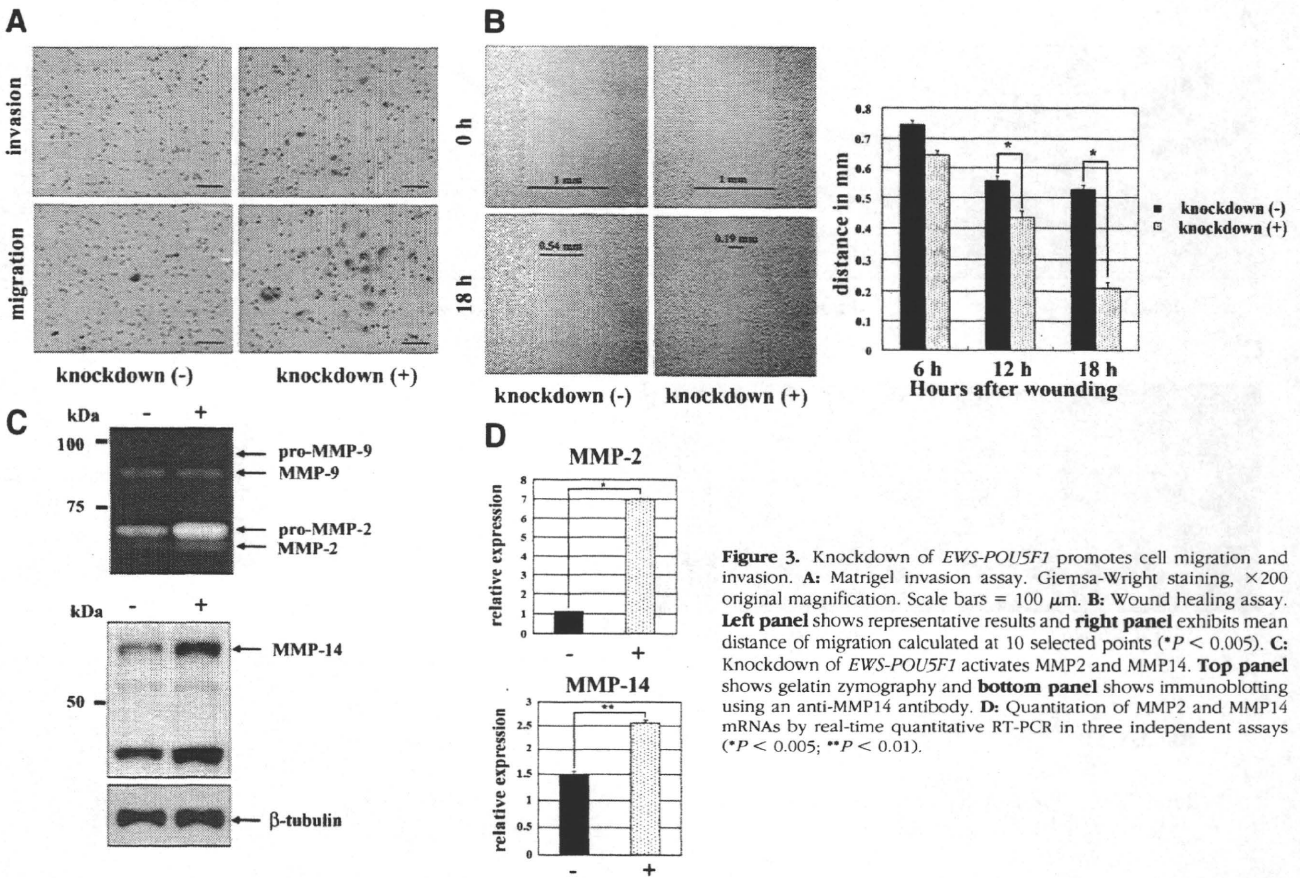
A

B

C

D

Figure 3. Knockdown of *EWS-POU5F1* promotes cell migration and invasion. **A:** Matrigel invasion assay. Giemsa-Wright staining, ×200 original magnification. Scale bars = 100 μm. **B:** Wound healing assay. **Left panel** shows representative results and **right panel** exhibits mean distance of migration calculated at 10 selected points (*$P < 0.005$). **C:** Knockdown of *EWS-POU5F1* activates MMP2 and MMP14. **Top panel** shows gelatin zymography and **bottom panel** shows immunoblotting using an anti-MMP14 antibody. **D:** Quantitation of MMP2 and MMP14 mRNAs by real-time quantitative RT-PCR in three independent assays (*$P < 0.005$; **$P < 0.01$).

regulate MMP expression directly or indirectly. The Matrigel invasion assay was also performed by using HeLa cells after introduction of the *EWS-POU5F1* expression vector. Cellular invasiveness was again suppressed (Figure 4A and Table 1; $P < 0.01$), though cell migration was decreased only moderately. In addition, depletion of MMP14 protein was demonstrated by introduction of *EWS-POU5F1* into both HeLa and HCT116 colon carcinoma cells (Figure 4B). Overexpression of *EWS-POU5F1* did not affect the expression level of p27, MMP2, or MMP9 in HeLa or HCT116 cells (data not shown). These results suggest that EWS-POU5F1 suppresses cellular motility and invasion in the broad cellular context. In contrast, overexpression of *p27^Kip1* did not affect either cell migration or invasion (Table 1), clearly indicating that cell motility/invasiveness is modulated in a p27-independent manner in GBS6 cells and that simple growth suppression is not sufficient to enhance the invasive activity of tumor cells.

Modulation of the Gene Expression Profile by EWS-POU5F1 Suppression

To investigate important downstream molecules regulated by EWS-POU5F1, alteration of global gene expression profiles by *EWS-POU5F1* knockdown was examined. We compared RNAs derived from *POU5F1*-specific siRNA-treated and control GBS6 cells (4 days after siRNA treatment) by using 54,676 probe sets of Affymetrix GeneChip Human Genome U133 Plus 2.0. We identified 98 probe sets (80 genes), the expression of which was increased more than 1.5-fold, and 55 probe sets (45 genes), the expression of which was decreased more than 1.5-fold (Figure 5A and Supplemental Table S1 at *http://ajp.amjpathol.org*). The genes whose expression was modified significantly were then classified according to gene ontology categories (Figure 5B). Interestingly,

Table 1. Invasiveness and Migration of GBS6 and HeLa Cells

Cells and treatment	EWS-POU5F1 knockdown in GBS6		p27 expression in GBS6		EWS-POU5F1 expression in HeLa	
	−	+	−	+	−	+
No. invasion	0.3 ± 0.4	101 ± 19*	0	0	1108 ± 85	357 ± 64*
No. migration	9.3 ± 3.2	>500*	11.1 ± 1.1	3.0 ± 0.7	3628 ± 401	1725 ± 229

Mean values ± SE of cell numbers of invasion and migration per 5×10^5 cells are exhibited.
*$P < 0.01$ versus control (−).

A

B

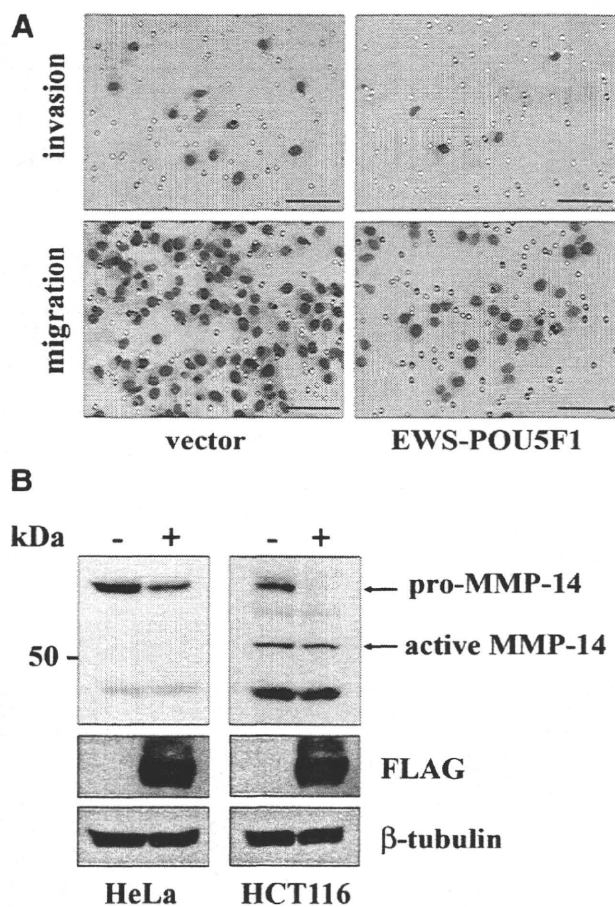**Figure 4.** Inhibition of cell migration and invasion by EWS-POU5F1 in HeLa cells. **A:** Matrigel invasion assay. Giemsa-Wright staining, ×200 original magnification. Scale bars = 100 μm. **B:** Immunoblotting of HeLa cells transfected with control (−) or *EWS-POU5F1* (+) expression vectors using anti-MMP14 (**top**), anti-FLAG (**middle**), and anti-β-tubulin (**bottom**).

23.8% of up-regulated genes were involved in cell motility, invasion, or cytoskeleton, consistent with the remarkable alteration of the phenotypes in GBS6 cells. In addition, 13.3% of down-regulated and 13.8% of up-regulated genes belong to differentiation and development categories, indicating importance of the POU5F1 function in pluripotency. However, *EWS-POU5F1* knockdown did not induce GBS6 cells to differentiate toward any specific lineage.

Representative differentially expressed genes of interest belonging to motility, adhesion/invasiveness, morphology/cytoskeleton, mesodermal differentiation, and growth suppression categories are shown in Figure 5C. In motility and adhesion/invasiveness categories, up-regulation of *MMP2* was again observed, though *MT1-MMP* was up-regulated only marginally. We also noted up-regulation of *CAV1*, the mutation of which is associated with mammary carcinoma invasiveness.[22] In addition, another up-regulated gene, *F2R*, has been reported as overexpressed in human cancers with high metastatic potency.[23] Down-regulation of *ELMO1* is intriguing because it is required for promoting phagocytosis and cell shape changes.[24]

A number of genes involved in the differentiation process were up-regulated by *EWS-POU5F1* knockdown.

MGP, LBH, JUN, MYOF, CTGF, and *MESDC2* are involved in mesodermal differentiation (Figure 5C and Supplemental Table S1 at *http://ajp.amjpathol.org*). The mesodermal origin of t(6;22) sarcoma was also supported by the fact that a number of genes encoding extracellular matrix proteins were also up-regulated. However, any specific differentiation toward muscle, bone, cartilage, or adipocytes was not supported by gene expression profiling.

Four putative tumor suppressors, *IGFBP7, HTRA1, TGFBR2,* and *SOCS3,* were up-regulated by *EWS-POU5F1* knockdown.[25–28] Although it remains unclear whether these genes are the direct targets of EWS-POU5F1, modified expression of these genes should be noted in addition to the altered state of p27, cyclin D1, and Rb. In summary, expression profiling provided important information on the molecular networks affected by the oncogenic function of EWS-POU5F1.

EWS-POU5F1 Up-Regulates the ES Cell-Specific miR302-367 Cluster

MicroRNAs (miRNAs) are noncoding RNAs consisting of approximately 22 nucleotides, which posttranscriptionally regulate mRNAs. They are important in development and differentiation, and abnormal expression of miRNAs has been reported in various neoplasms.[29,30] The miR302-367 cluster has been identified recently as ES cell-specific, and the cluster is transcriptionally regulated by Nanog, POU5F1, Sox2, and Rex1.[31,32] RT-PCR analysis revealed remarkable down-regulation of the miR302-367 cluster during knockdown of *EWS-POU5F1* (Figures 6A and 6B), suggesting that chimeric EWS-POU5F1, like wild-type POU5F1, may regulate miR302-367. The result strongly suggests that EWS-POU5F1 regulates downstream genes not only by its direct DNA binding but also through modulating the expression of miRNA.

Discussion

In the present study we show that EWS-POU5F1 enhances cellular proliferation of GBS6 sarcoma cells. Knockdown of *EWS-POU5F1* caused GBS6 cells to arrest in the G1 phase of the cell cycle. We also noted up-regulation of p27^{Kip1}, down-regulation of cyclin D1, and diminished phosphorylation of Rb protein. The tumor suppressor p27^{Kip1} is a CDK2 inhibitor, and it inhibits the cell cycle at the G1/S transition.[33] It is likely that p27^{Kip1} functions downstream from EWS-POU5F1 in oncogenic transformation. In support of this idea, exogenous introduction of p27^{Kip1} blocked proliferation of GBS6 cells.

During suppression of *EWS-POU5F1*, GBS6 cells showed morphological changes similar to those seen in cellular senescence (eg, spreading of the cytoplasm, marked enlargement of cell size, and expression of senescence-associated β-galactosidase, a hallmark of senescence).[15] However, the lack of senescence-associated heterochromatin foci[16] and the reversible nature of the G1 arrest suggest that the change induced by *EWS-POU5F1* knockdown differs from senescence. Loss of p16^{INK4A} might protect GBS6 cells from senescence,

A

B

Up-regulated genes

GO annotations

- Motility/invasion/cytoskeleton
- Differentiation/development
- Signaling pathways
- Transcription
- Cell cycle
- Apoptosis
- Transport
- Miscellaneous

Down-regulated genes

C

IGFBP7 (10.1)		THBS1 (5.38)
HTRA1 (2.78)		CAV1 (2.25)
TGFBR2 (2.18)		CDC42EP3 (1.66)
SOCS3 (1.91)		ELMO1 (-2.43)
Growth suppression		Morphology/Cytoskeleton

EWS-POU5F1

Mesodermal differentiation

| MGP (70.55) |
| LBH (16.00) |
| JUN (2.29) |
| MYOF (2.20) |
| CTGF (2.09) |
| MESDC2 (1.59) |

Motility

| THBS1 (5.38) |
| F2R (2.73) |
| CTGF (2.09) |
| TPM1 (1.59) |
| LAMB1 (1.57) |

Adhesion/Invasiveness

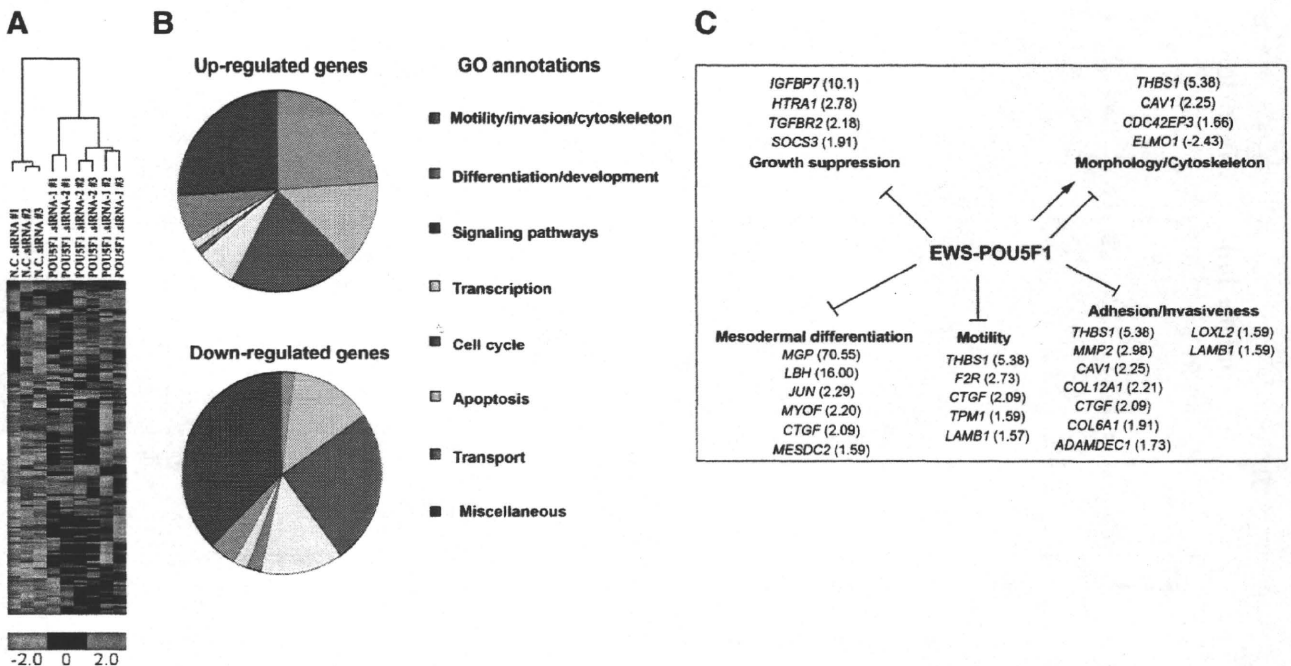| THBS1 (5.38) | LOXL2 (1.59) |
MMP2 (2.98)	LAMB1 (1.59)
CAV1 (2.25)	
COL12A1 (2.21)	
CTGF (2.09)	
COL6A1 (1.91)	
ADAMDEC1 (1.73)	

-2.0 0 2.0

Figure 5. Gene clustering analysis across the compared populations. **A:** Heat map shows the expression of EWS-POU5F1 regulated genes in GBS6 cells treated with negative control siRNA or *POU5F1*-specific siRNAs. Up-regulated and down-regulated genes are presented in red and green, respectively. **B:** Pie charts show the distribution of the 80 up-regulated and 45 down-regulated genes in GBS6 cells transfected with *POU5F1* siRNAs according to gene ontology (GO) annotations. **C:** Prediction of the major signaling pathways affected by EWS-POU5F1. Lower bound of fold changes in each gene are indicated in parentheses.

and senescence-like morphological changes might be achieved by alteration of the actin fiber network.

The inhibitory role of EWS-POU5F1 in cell migration and invasion was unexpected. It is very likely that multiple

A   M   -   +   ddw

miR302-367

β-actin

B   miR302-367

Figure 6. A: RT-PCR analysis of miR302-367 in GBS6 cells transfected with control (−) or POU5F1 (+). β-actin was amplified to confirm qualities and quantities of RNA. **B:** Real time quantitative RT-PCR analysis of miR302-367. Average expression was calculated in three independent experiments ($*P < 0.005$).

molecular processes were responsible for increased motility and invasiveness of GBS6 cells treated with *POU5F1* siRNAs. It has been reported that RhoA activation induces actin polymerization[17] that is causatively related to cancer cell invasion and migration.[34] Paradoxical promotion of tumor invasiveness related to p27[Kip1]-dependent G1 arrest has been reported in malignant melanoma with Mitf activation in which Mitf promotes melanoma proliferation by down-regulating p27[Kip1] but suppresses tumor cell invasion by the Dia1-dependent pathway.[35] Furthermore, p27[Kip1] supports cell motility through modulation of the RhoA pathway.[36] In GBS6 cells, however, introduction of p27[Kip1] affected neither cell mobility/invasiveness nor morphological changes. Those results suggest that there might be a p27[Kip1]-independent pathway in RhoA activation and actin polymerization. MMP2 and MT1-MMP, which were up-regulated by knockdown of *EWS-POU5F1*, are candidate upstream regulators of RhoA because recent studies indicate these MMPs induce RhoA activation in osteosarcoma and vascular endothelial cells.[37,38] Moreover, our study indicates that increased cell motility was not a simple consequence of growth suppression. Furthermore, the present results raise an important concern for the treatment of cancer in general. That is, when treatment suppresses the expression of oncogenic transcription factors, inhibition of tumor growth might be accompanied by enhanced tumor cell invasion and metastasis.

Carcinogenesis is a multistep process that requires multiple genetic and epigenetic alterations.[39] Therefore, the fusion of *EWSR1* and *POU5F1* is not sufficient for complete carcinogenesis, and t(6;22) tumors possess additional mutations such as *p16/p14* loss. Our prelimi-
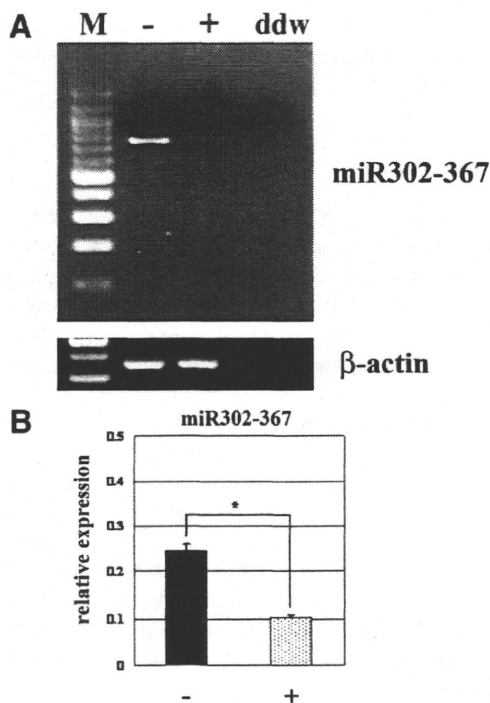
nary study demonstrated that retrovirus-mediated gene transfer of *EWS-POU5F1* could immortalize but not induce full transformation of murine mesenchymal stem cells (M. Tanaka and T. Nakamura, unpublished observation). Identification of genes cooperative with *EWS-POU5F1* for carcinogenesis is important, and genetic analysis including mutagenesis experiments will provide useful information for understanding the mechanism of *POU5F1*-induced carcinogenesis. In addition, our study suggests that tumor progression toward invasive properties may be caused by genes that do not cooperate with *EWS-POU5F1* but may even counteract *EWS-POU5F1*.

It is intriguing to define important EWS-POU5F1 target genes in carcinogenesis. Because POU5F1/Oct3/4 is a transcriptional regulator, it is likely that the fusion to EWS modulates the nature of its regulatory activities for downstream target genes. Previous studies suggested that POU5F1 acquires the enhanced transcriptional activity by addition of the EWS N-terminal domain.[13,40] The target genes for POU5F1 have been extensively investigated by using ES cells.[4,41,42] In these studies POU5F1 is found associated with SOX2 and/or Nanog, both of which are also expressed in GBS6 cells (data not shown). However, the down-regulated genes in *EWS-POU5F1* knockdown GBS6 cells did not always overlap with POU5F1 target genes in ES cells, probably because of the different cellular context between ES cells and sarcoma cells. Alternatively, the addition of the EWS N-terminal domain may alter the binding specificity of POU5F1 to the target sequences. Nevertheless, it is still possible that there are common target genes for both EWS-POU5F1 and wild-type POU5F1. In a comparison between genes showing altered expression on *EWS-POU5F1* knockdown in the present study and the genes detected in chromatin immunoprecipitation (ChIP)-on-chip or chromatin immunoprecipitation-paired-end ditag (ChIP-PET) studies,[41,42] *INSIG1*, *EPHA4*, *DHCR7*, *ANKS1B*, *ANO4*, *RDH10*, *PHF19*, *BNIP3*, and *TRIB1* are good candidates for common target genes of POU5F1 or EWS-POU5F1 in organogenesis or sarcomagenesis. In addition, the miR302-367 cluster has been identified as a target of ES cell-associated transcription factors, including POU5F1.[32] Down-regulation of miR302-367 on *EWS-POU5F1* knockdown strongly suggests that EWS-POU5F1 regulates gene expression by recognition of a target sequence as well as miRNA-mediated mRNA inhibition. In fact, overexpression of miR302 induces cell cycle progression of ES cells.[43] Interestingly, miR302 represses protein expression of cyclin D1 in ES cells, the opposite effect for EWS-POU5F1 in GBS6 cells, suggesting cell context-dependent function of the miR302-467 cluster. Further studies are needed to identify key downstream molecules controlling cell proliferation and/or cell motility and invasiveness.

Acknowledgments

References

1. Schöler HR, Dressler GR, Balling R, Rohdewohld H, Gruss P: Oct-4: a germline-specific transcription factor mapping to the mouse t-complex. EMBO J 1990, 9:2185–2195

2. Nichols J, Zevnik B, Anastassiadis K, Niwa H, Klewe-Nebenius D, Chambers I, Schöler H, Smith A: Formation of pluripotent stem cells in the mammalian embryo depends on the POU transcription factor Oct4. Cell 1998, 95:379–391

3. Niwa H, Miyazaki J, Smith AG: Quantitative expression of Oct-3/4 defines differentiation, dedifferentiation or self-renewal of ES cells. Nat Genet 2000, 24:372–376

4. Matoba R, Niwa H, Masui S, Ohtsuka S, Carter MG, Sharov AA, Ko MS: Dissecting Oct3/4-regulated gene networks in embryonic stem cells by expression profiling. PLoS ONE 2006, 1:e26

5. Ivanova N, Dobrin R, Lu R, Kotenko I, Levorse J, DeCoste C, Schafer X, Lun Y, Lemischka IR: Dissecting self-renewal in stem cells with RNA interference. Nature 2006, 442:533–538

6. Takahashi K, Yamanaka S: Induction of pluripotent stem cells from mouse embryonic and adult fibroblast cultures by defined factors. Cell 2006, 126:1–14

7. Kim JB, Zaehres H, Wu G, Gentile L, Ko K, Sebastiano V, Araúzo-Bravo MJ, Ruau D, Han DW, Zenke M, Schöler HR: Pluripotent stem cells induced from adult neural stem cells by reprogramming with two factors. Nature 2008, 454:646–650

8. Jin T, Branch DR, Zhang X, Qi S, Youngson B, Goss PE: Examination of POU homeobox genes in breast cancer cells. Int J Cancer 1999, 81:104–112

9. Gidekel S, Pizov G, Bergman Y, Pikarsky E: Oct3/4 is a dose-dependent oncogenic fate determinant. Cancer Cell 2003, 4:361–370

10. Looijenga LH, Stoop H, de Leeuw HP, de Gouveia Brazao CA, Gillis AJ, van Roozendaal KE, van Zoelen EJ, Weber RF, Wolffenbuttel KP, van Dekken H, Honecker F, Bokemeyer C, Perlman EJ, Schneider DT, Kononen J, Sauter G, Oosterhuis JW: POU5F1 (OCT3/4) identifies cells with pluripotent potential in human germ cell tumors. Cancer Res 2003, 63:2244–2250

11. Atlasi Y, Mowla SJ, Ziaee SA, Bahrami AR: OCT-4, an embryonic stem cell marker, is highly expressed in bladder cancer. Int J Cancer 2007, 120:1598–1602

12. Yamaguchi S, Yamazaki Y, Ishikawa Y, Kawaguchi N, Mukai H, Nakamura T: EWSR1 is fused to POU5F1 in a bone tumor with translocation t(6;22)(p21;q12). Genes Chromosomes Cancer 2005, 43:217–222

13. Möller E, Stenman G, Mandahl N, Hamberg H, Mölne L, van den Oord JJ, Brosjö O, Mertens F, Panagopoulos I: POU5F1, encoding a key regulator of stem cell pluripotency, is fused to EWSR1 in hidradenoma of the skin and mucoepidermoid carcinoma of the salivary glands. J Pathol 2008, 215:78–86

14. Kawamura-Saito M, Yamazaki Y, Kaneko K, Kawaguchi N, Kanda H, Mukai H, Gotoh T, Motoi T, Fukayama M, Aburatani H, Takizawa T, Nakamura T: Fusion between CIC and DUX4 up-regulates PEA3 family genes in Ewing-like sarcomas with t(4;19)(q35;q13) translocation. Hum Mol Genet 2006, 15:2125–2137

15. Lundberg AS, Hahn WC, Gupta P, Weinberg RA: Genes involved in senescence and immortalization. Curr Opin Cell Biol 2000, 12:705–709

16. Narita M, Núñez S, Heard E, Narita M, Lin AW, Hearn SA, Spector DL, Hannon GJ, Lowe SW: Rb-mediated heterochromatin formation and silencing of E2F target genes during cellular senescence. Cell 2003, 113:703–716

17. Ridley AJ, Hall A: The small GTP-binding protein rho regulates the assembly of focal adhesions and actin stress fibers in response to growth factors. Cell 1992, 70:401–410

18. Hanahan D, Weinberg RA: The hallmarks of cancer. Cell 2000, 100:57–70

19. Seiki M: The cell surface: the stage for matrix metalloproteinase regulation of migration. Curr Opin Cell Biol 2002, 14:624–635

20. Seiki M, Mori H, Kajita M, Uekita T, Itoh Y: Membrane-type 1 matrix metalloproteinase and cell migration. Biochem Soc Symp 2003, 70:253–262

21. Seiki M, Koshikawa N, Yana I: Role of pericellular proteolysis by membrane-type 1 matrix metalloproteinase in cancer invasion and angiogenesis. Cancer Metastasis Rev 2003, 22:129–143

22. Bonuccelli G, Casimiro MC, Sotgia F, Wang C, Liu M, Katiyar S, Zhou J, Dew E, Capozza F, Daumer KM, Minetti C, Milliman JN, Alpy F, Rio MC,

Tomasetto C, Mercier I, Flomenberg N, Frank PG, Pestell RG, Lisanti MP: Caveolin-1 (P132L), a common breast cancer mutation, confers mammary cell invasiveness and defines a novel stem cell/metastasis-associated gene signature. Am J Pathol 2009, 174:1650–1662

23. Boire A, Covic L, Agarwal A, Jacques S, Sherifi S, Kuliopulos A: PAR1 is a matrix metalloprotease-1 receptor that promotes invasion and tumorigenesis of breast cancer cells. Cell 2005, 120:303–313

24. Gumienny TL, Brugnera E, Tosello-Trampont AC, Kinchen JM, Haney LB, Nishiwaki K, Walk SF, Nemergut ME, Macara IG, Francis R, Schedl T, Qin Y, Van Aelst L, Hengartner MO, Ravichandran KS: CED-12/ELMO, a novel member of the CrkII/Dock180/Rac pathway, is required for phagocytosis and cell migration. Cell 2001, 107:27–41

25. Wilson EM, Oh Y, Hwa V, Rosenfeld RG: Interaction of IGF-binding protein-related protein 1 with a novel protein, neuroendocrine differentiation factor, results in neuroendocrine differentiation of prostate cancer cells. J Clin Endocr Metab 2001, 86:4504–4511

26. Chien J, Staub J, Hu SI, Erickson-Johnson MR, Couch FJ, Smith DI, Crowl RM, Kaufmann SH, Shridhar V: A candidate tumor suppressor HtrA1 is downregulated in ovarian cancer. Oncogene 2004, 23:1636–1644

27. Markowitz S, Wang J, Myeroff L, Parsons R, Sun L, Lutterbaugh J, Fan RS, Zborowska E, Kinzler KW, Vogelstein B, Brattain M, Willson JKV: Inactivation of the type II TGF-beta receptor in colon cancer cell with microsatellite instability. Science 1995, 268:1336–1338

28. He B, You L, Uematsu K, Zang K, Xu Z, Lee AY, Costello JF, McCormick F, Jablons DM: SOCS-3 is frequently silenced by hypermethylation and suppresses cell growth in human lung cancer. Proc Natl Acad Sci USA 2003, 100:14133–14138

29. Lagos-Quintana M, Rauhut R, Yalcin A, Meyer J, Lendeckel W, Tuschl T: Identification of tissue-specific microRNAs from mouse. Curr Biol 2002, 12:735–739

30. Aravin AA, Lagos-Quintana M, Yalcin A, Zavolan M, Marks D, Snyder B, Gaasterland T, Meyer J, Tuschl T: The small RNA profile during Drosophila melanogaster development. Dev Cell 2003, 5:337–350

31. Suh MR, Lee Y, Kim JY, Kim SK, Moon SH, Lee JY, Cha KY, Chung HM, Yoon HS, Moon SY, Kim VN, Kim KS: Human embryonic stem cells express a unique set of microRNAs. Dev Biol 2004, 270:488–498

32. Barroso-del Jesus A, Romero-López C, Lucena-Aguilar G, Melen GJ, Sanchez L, Ligero G, Berzal-Herranz A, Menendez P: Embryonic stem cell-specific miR302-367 cluster: human gene structure and functional characterization of its core promoter. Mol Cell Biol 2008, 28:6609–6619

33. Sherr CD, Roberts JM: CDK inhibitors: positive and negative regulators of G1-phase progression. Genes Dev 2001, 13:1501–1512

34. Yamaguchi H, Condeelis J: Regulation of the actin cytoskeleton in cancer cell migration and invasion. Biochim Biophys Acta 2007, 1773:642–652

35. Carreira S, Goodall J, Denat L, Rodriguez M, Nuciforo P, Hoek KS, Testori A, Larue L, Goding CR: Mitf regulation of Dia1 controls melanoma proliferation and invasiveness. Genes Dev 2006, 20:3426–3439

36. Fromique O, Hamidouche Z, Marie PJ: Nlockade of the RhoA-JNK-c-Jun-MMP2 cascade by atorvastatin reduces osteosarcoma cell invasion. J Biol Chem 2008, 283:30549–30556

37. Sugimoto K, Ishibashi T, Sawamura T, Inoue N, Kamioka M, Uekita H, Ohkawara H, Sakamoto T, Sakamoto N, Okamoto Y, Takuwa Y, Kakino A, Fujita Y, Tanaka T, Teramoto T, Maruyama Y, Takeishi Y: LOX-1-MT1-MMP axis is crucial for RhoA and Rac1 activation induced by oxidized low-density lipoprotein in endothelial cells. Cardiovasc Res 2009, 84:127–136

38. Besson A, Gurian-West M, Schmidt A, Hall A, Roberts JM: p27Kip1 modulates cell migration through the regulation of RhoA activation. Genes Dev 2004, 18:862–876

39. Weinberg RA: Multistep tumorigenesis: the biology of cancer. Edited by RA Weinberg. Garland Science, New York, NY 2007, pp 399–462

40. Lee J, Kim JY, Kang IY, Kim HK, Han YM, Kim J: The EWS-Oct-4 fusion gene encodes a transforming gene. Biochem J 2007, 406:519–526

41. Boyer LA, Lee TI, Cole MF, Johnstone SE, Levine SS, Zucker JP, Guenther MG, Kumar RM, Murray HL, Jenner RG, Gifford DK, Melton DA, Jaenisch R, Young RA: Core transcriptional regulatory circuitry in human embryonic stem cells. Cell 2005, 122:947–956

42. Loh YH, Wu Q, Chew JL, Vega VB, Zhang W, Chen X, Bourque G, George J, Leong B, Liu J, Wong KY, Sung KW, Lee CW, Zhao XD, Chiu KP, Lipovich L, Kuznetsov VA, Robson P, Stanton LW, Wei CL, Ruan Y, Lim B, Ng HH: The Oct4 and Nanog transcription network regulates pluripotency in mouse embryonic stem cells. Nat Genet 2006, 38:431–440

43. Greer Card DA, Hebbar PB, Li L, Trotter KW, Komatsu Y, Mishina Y, Archer TK: Oct4/Sox2-regulated miR-302 targets cyclin D1 in human embryonic stem cells. Mol Cell Biol 2008, 28:6426–6438

RESEARCH PAPER

Lung cancer progression and metastasis from the prognostic point of view

Kentaro Inamura · Yuichi Ishikawa

Abstract Lung cancer is the leading cause of cancer death in men and women worldwide. Since the occurrence of metastases in distant organs is the major reason for mortality of cancer patients, we need to elucidate the underlying mechanisms. Many studies featuring analysis of gene expression, comparative genomic hybridization and loss of heterozygosity analysis have been performed and generated support for the hypothesis that metastatic potential is acquired early in tumorigenesis. Furthermore, it is now clear that the majority of tumor cells have the potential to metastasize. Although many changes in gene expression profiles have been established retrospectively, translational research is now a high priority to enable clinical application and treatment based on laboratory findings.

Introduction

Lung cancer, the leading cause of cancer death in men and women worldwide and continuing to rise in frequency, is generally classified as of either small-cell lung carcinoma (SCLC) or non-SCLC (NSCLC) types. Within these groups further distinctions are made, with NSCLCs sub-divided into adenocarcinomas, squamous cell carcinomas (SCCs), and

large cell carcinomas (LCCs). The occurrence of metastases in distant organs is the major cause of death for the vast majority of lung cancer patients. Clinical outcomes can be roughly predicted by pathological-Stage (p-Stage) and 5 year survival for p-Stage I cases, pathologically lacking metastases, is relatively good, ranging from 60 [1] to 90% [2]. Even when cancer lesions have been fully removed and no metastasis is found at surgery, however, some patients with p-Stage I lesions suffer recurrence and die of cancer relapse. Presumably, these already had micrometastases at the time of tumor removal. To avoid unnecessary lymph node dissection in low-risk cases but ensure that postoperative adjuvant therapy is performed for high-risk patients, we need a clinically useful approach to better stratify patients with respect to the risk of recurrence. Towards a rational treatment, we need to elucidate metastatic gene signatures and molecular mechanisms of lung cancer progression. The aim of the present review is to survey findings on lung cancer progression and metastasis from the prognostic point of view, especially emphasizing our study [3] paying attention to heterogeneity of lung cancers, an important characteristic.

The beginning of gene expression profiling in lung cancers

In November, 2001, pioneering studies of gene expression profiling in lung cancers were reported at the same time by a Stanford University group [4] and a Harvard University group [5]. Subdivision of the tumors based on gene expression faithfully recapitulated their histological classification and characteristic expression profiles for each histological type could be identified. The insulinoma-associated gene 1 (IA-1) and the human achaetescute homolog 1 (hASH1) were found to be neuroendocrine SCLC markers, shared also

K. Inamura · Y. Ishikawa (✉)
Department of Pathology, The Cancer Institute, Japanese
Foundation for Cancer Research (JFCR), 3-10-6 Ariake,
135-8550 Koto-ku, Tokyo, Japan
e-mail: ishikawa@jfcr.or.jp

⌀ Springer

by carcinoid tumors. Identified as SCC markers were Keratin 5 (KRT5), KRT17 and Tumor protein p63, which is associated with development of squamous epithelium. Supporting the traditional view that lung adenocarcinomas are a heterogeneous group, distinct subclasses were evident. One adenocarcinoma subgroup was comprised of tumors expressing neuroendocrine markers, such as hASH1 and IA-1, associated with a significant decrease in patient survival when compared to other adenocarcinomas [5]. Another subgroup appeared to express markers of alveolar type II pneumocytes and was characterized by high relative expression of TTF1 or surfactant protein genes.

Gene expression profiling predicting survival of patients with lung adenocarcinomas

As mentioned above, the Stanford University group [4] and the Harvard University group [5] first identified prognostically different subgroups of adenocarcinomas by gene expression profiling. One subgroup with a poor prognosis was revealed to have neuroendocrine features. Subsequently, many further studies using gene expression profiling have been reported. Beer et al. [6] described development of a risk index, compiling the relative expression of 50 genes, to identify high or low risk groups of Stage I adenocarcinomas that correlated with patient survival.

Ramaswamy et al. [7] compared gene expression profiles of adenocarcinoma metastases and unmatched primary adenocarcinomas and found patterns that allowed distinction between the two, but also reported that a subset of primary tumors had similar expression to metastases. This finding led them to challenge "the notion that metastases arise from rare cells within the primary tumor." They suggested that the majority of tumor cells have the potential to metastasize, but this remains controversial and Liotta and Kohn have argued against their conclusions [8]. When lists of genes are examined, it is unclear whether the expression profile is a cause or a local consequence of the metastatic process. Ramaswamy et al. did not microdissect tumor cells for analysis of their tissue specimens and consequently the gene-expression pattern data reflect contributions from multiple cell populations. Thus, the expression pattern of the genes in the authors' signature set may be at least partially due to activated host stromal elements. Indeed, two of the important upregulated genes in the list encode stromal collagen.

Although gene expression profiles that can classify cancer patients according to the risk of recurrence have been found, most studies have been retrospective. Very recently, Potti et al. [9] documented a "lung metagene model" that can identify individuals at increased risk for disease recurrence with stage IA NSCLC, which they now plan to use for a prospective randomized clinical trial. Translational research

is now an urgent priority to enable clinical application of basic research findings.

Gene expression profiling using hierarchical clustering and non-negative matrix factorization in squamous cell carcinomas

After the adenocarcinoma, the SCC is the most frequent lung cancer histology, accounting for approximately 30% of the total. Its development is the most strongly related to smoking. For adenocarcinomas, subclassification by differentiation grade [10] or histological pattern [2] is useful to predict prognosis. For SCCs, differentiation grade is used for pathological subclassification, but it correlates poorly with prognosis. Although SCCs demonstrate some histological variation, such as with the basaloid variant, this does not allow good prediction of prognosis. The present system used to subclassify SCC is thus insufficient and we have therefore attempted to make a clinically useful classification based on gene expression profiling [11]. By hierarchial clustering, we subclassified SCCs into two prognostically significant subclasses. Furthermore, consensus clustering with a non-negative matrix factorization (NMF) approach indicated the robustness of this classification (Fig. 1). NMF appears to be more accurate for choice of input genes than hierarchial clustering and can be combined with a quantitative evaluation of the robustness with numbers of clusters [12]. Both hierarchical clustering and NMF approaches (Fig. 1) indicated that SCCs can be divided into two groups, SCC-A and SCC-B, with prognostic variation (Fig. 2a). The cophenetic correlation coefficient, k, quantitatively indicated the two-centroid clustering to be the most robust with the highest value, as attested by clear block diagonal patterns (Fig. 2b). Up-regulation of cell-proliferation-related genes was evident in the subclass with poor survival. In the subclass with better survival, genes involved in differentiated intracellular functions, such as the MAPKKK cascade, ceramide metabolism, or regulation of transcription, were upregulated.

Histological typing and gene expression profiles in high-grade neuroendocrine tumors

The current WHO classification of high-grade neuroendocrine tumors (HGNTs) currently recognizes large-cell neuroendocrine carcinoma (LCNEC), a subclass of LCC, and SCLC as a distinct group [13]. Since LCNEC and SCLC share several histological features, a consensus differential diagnosis between LCNEC and SCLC is sometimes difficult, even among experienced lung pathologists. Hence, by the microarray technique, we analyzed gene
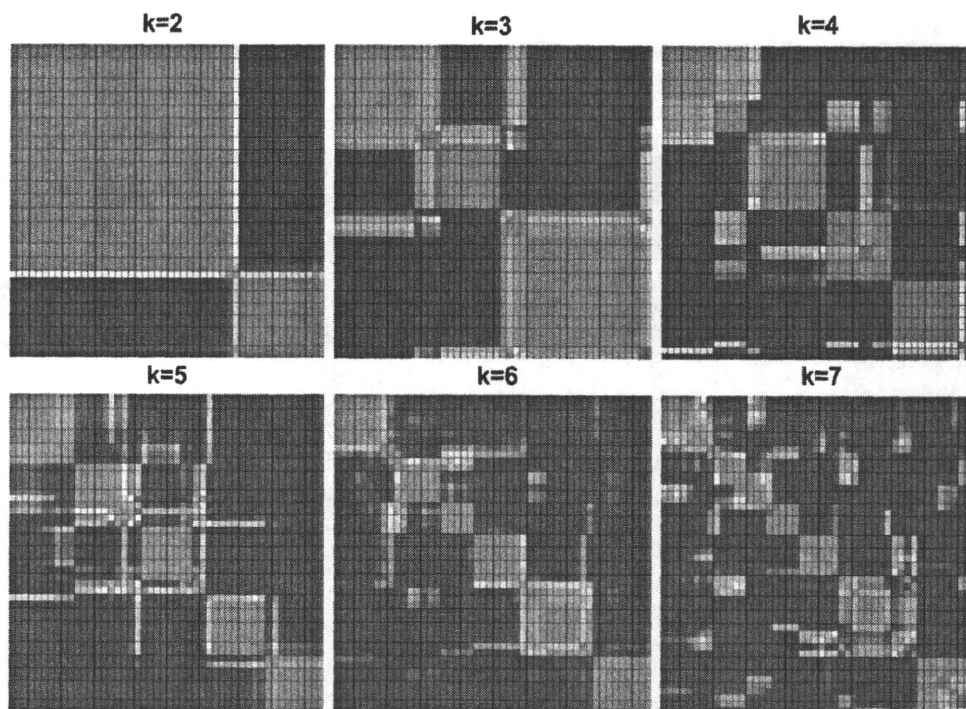
Fig. 1 Reordered consensus averaging 50 connectivity matrices computed at $k = 2$–7 for all SCC samples with 3,344 genes. Samples were hierarchically clustered, colored from 0 (samples never in the same cluster) to 1 (samples always in the same cluster)

Fig. 2 **a** Kaplan–Meier survival curves for the 48 SCC patients (SCC-A vs. SCC-B). **b** Cophenetic correlation coefficients for the hierarchically clustered matrices
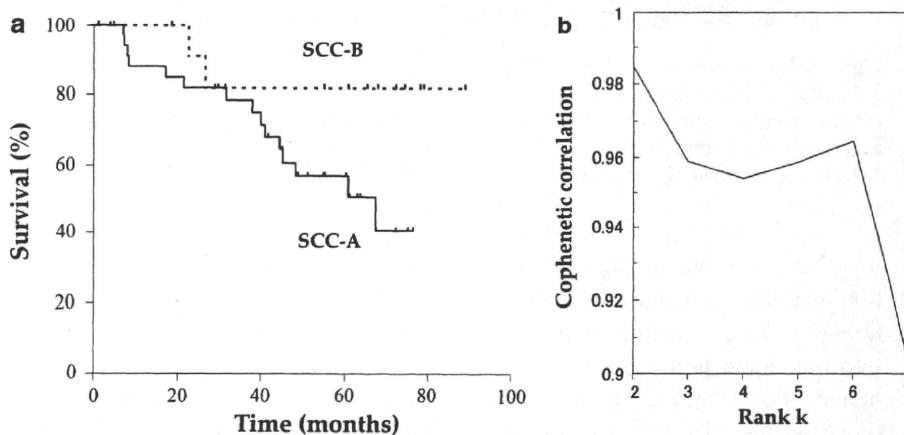
expression profiles of HGNTs with other histological tumor groups and normal lung tissue [14]. By hierarchical clustering, we could readily identify distinct groups for carcinoids, LCC, adenocarcinoma, and normal lung (Fig. 3a). While we could not subclassify SCLC and LCNEC by gene expression profiling, two prognostically significant subtypes of HGNT were evident, independent of SCLC and LCNEC ($P = 0.0094$). Many genes distinguished the HGNT groups. There was no significant difference in survival between SCLC and LCNEC samples (Fig. 3b; $P = 0.37$).

Integrated classification of lung tumors and cell lines by expression profiling

The utility of cancer cell lines depends largely on their accurate classification, commonly based on histopathological diagnosis of the cancers from whom they were derived. However, because cancers are often heterogeneous, cell lines, which also have a propensity to alter in vitro, may not be truly representative. We therefore performed gene expression profiling, which can faithfully recapitulate histological classification of tumors, to examine different cell
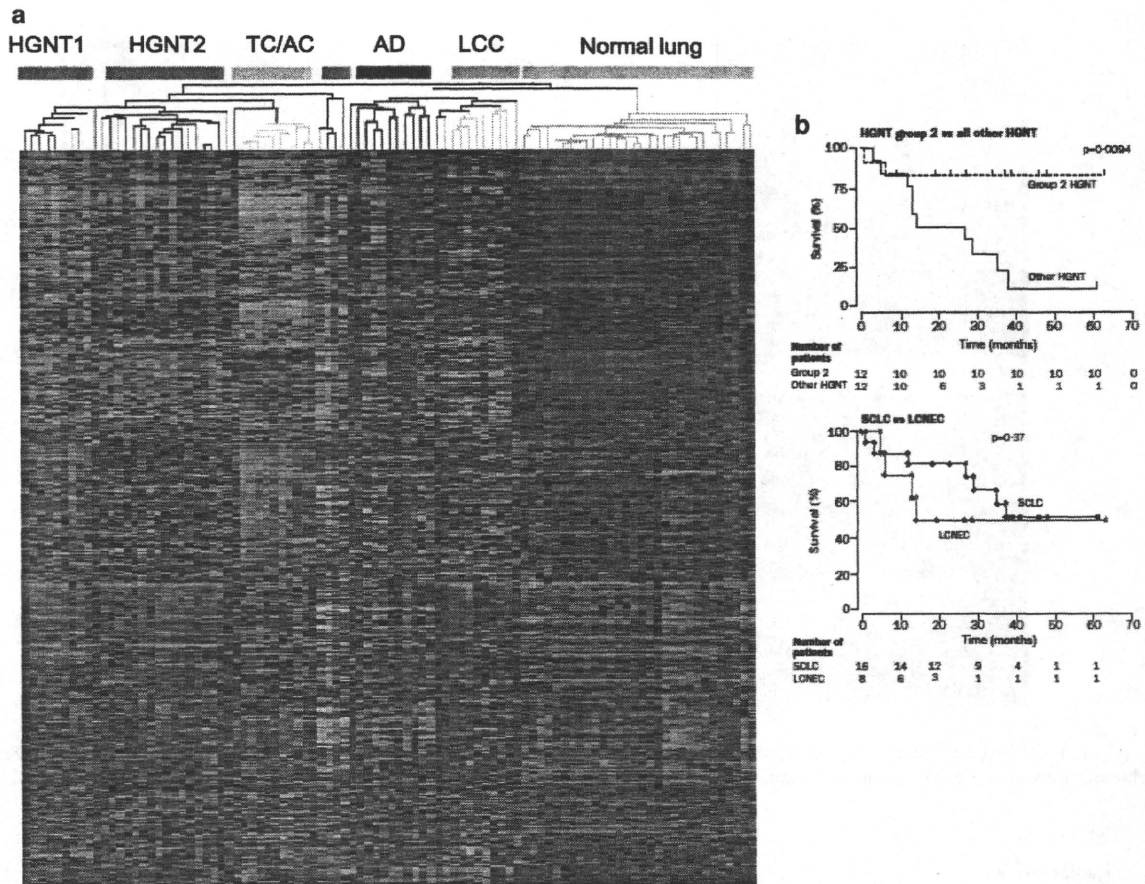
Fig. 3 a Unsupervised hierarchical clustering of 64 lung cancer and 30 normal lung samples against 2,803 genes with expression differentially regulated in neuroendocrine tumors. *HGNT* high grade neuroendocrine tumor, *TC/AC* typical carcinoids/atypical carcinoids, *AD* adenocarcinoma, *LCC* large cell carcinoma. **b** Kaplan-Meyer survival curves for patients with HGNTs in group 2 and all other HGNTs and for histopathologically diagnosed SCLC versus LCNEC. SCLC, small-cell lung carcinoma; LCNEC, large-cell neuroendocrine carcinoma

lines [15]. After excluding genes which show clear distinction between fresh and cell-line samples, hierarchical clustering resulted in a large degree of integration of cell lines into four main tumor branches, an SCLC branch, a SCC branch, a cell-line branch, and a branch containing normal tissue, adenocarcinoma and LCC (Fig. 4). As a result, most of SCC cell lines or SCLC cell lines grouped with fresh SCC tumors or fresh SCLC tumors, respectively. In contrast, although none of adenocarcinoma cell lines clustered with fresh adenocarcinoma tumors, some of them clustered with fresh SCC tumors or fresh SCLC tumors. Adenocarcinomas may ultimately progress toward one of two poorly differentiated phenotypes with expression profiles resembling SCC or SCLC. Our observations suggest that adenocarcinoma cell lines either dedifferentiate toward molecular pathologies resembling SCLC or SCC, or that clonal expansion of SCC or SCLC subcomponents occurs frequently. Analysis of larger numbers of adenocarcinoma samples taken at the time of surgery and autopsy will be required to verify that adenocarcinomas develop similarly in situ.

Comparison of accumulated allele loss between primary lung tumors and lymph node metastases

Sasatomi et al. [16] have compared loss of heterozygosity (LOH) at microsatellites between primary NSCLCs and their lymph node metastases, calculating fractional allele loss (FAL), defined as the ratio of chromosomes affected by LOH in the informative chromosomes, for each sample. With Stage II NSCLCs, the FAL was found to be significantly less in the metastatic sites compared with the primary neoplasms. The authors advanced the theory that this phenomenon was the result of early metastatic spread of the carcinoma, with the primary neoplasm then acquiring additional genetic changes. This concept should be borne in mind when comparing molecular profiles of
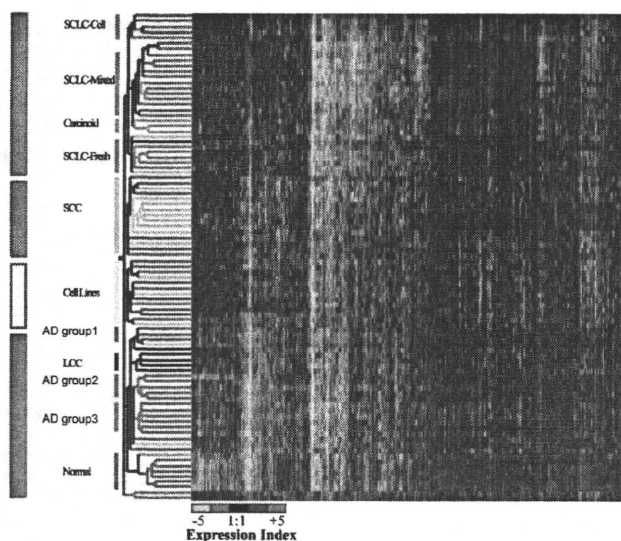
Fig. 4 Dendrogram of the reduced data set of 4,253 genes after filtering for commonly regulated genes in either fresh or cell-line samples. Groupings indicated on the *left* represent distinct clusters of particular carcinoma types. AD, adenocarcinoma; Normal, normal lung tissue

primary neoplasms with those of metastatic or recurrent sites.

Gene expression profile for tissue-specific metastasis

Kang et al. [17] have identified, in a human breast cancer cell line, a specific set of genes that mediates metastasis to bone. They suggested that primary tumors with metastatic capacity possess the poor-prognosis signature but, additional functions, provided by a set of bone metastasis genes, must be expressed in order to achieve an overt, tissue-specific metastasis phenotype. Organ-specific expression profiles for human small-cell lung cancer metastases in mice have also been reported by Kakiuchi et al. [18], but it remains unclear whether these might already be present in the parental cells.

Heterogeneity of primary tumors and metastatic potential

Introduction

Recent microarray experiments have suggested that the majority of cancer cells have the potential to metastasize, with obvious clinical and therapeutic implications, not only in breast cancers [19], but also in lung cancers [7]. Ramaswamy et al. [7] identified a molecular signature of metastatic potential within the bulk of each primary lung cancer, suggesting that metastatic potential is in fact

acquired early and is a feature of the majority of lung cancer cells. To test this hypothesis, we adopted the lung adenocarcinoma, which characteristically shows widespread intratumoral heterogeneity, as a model [3].

The mixed type adenocarcinoma in the lung, which shows a variety of histological subtypes, is the most frequent subtype in the WHO classification criteria [13], accounting for approximately 80% of resected lung adenocarcinomas [20]. An invasive component with high cellular and structural atypia is often included but peripherally well-differentiated components with low atypia may also be present (Fig. 5). Is the metastatic signature detected only in the aggressive component with high atypia? Or is it present in the entire tumor irrespective of morphological heterogeneity? If the latter is true, then it follows that the metastatic potential is acquired early in tumor progression and the entire tumor, including the morphologically less malignant component, may have metastatic potential.

Using lymph node-positive lung adenocarcinomas, we compared gene expression profiles among moderately-differentiated components with aggressive appearance, peripheral well-differentiated components with less malignant appearance, and patient-matched lymph node metastases. Node-negative lung adenocarcinomas, which are morphologically indistinguishable from node-positive tumors, were included for comparison and differential diagnosis.

Schematic design

The schematic design for this study is shown in Fig. 5. We analyzed 10 pairs of primary lung adenocarcinomas and their synchronous lymph node metastases and 11 primary lung adenocarcinomas without lymph node or organ metastases. With the 21 primary lung adenocarcinomas, we isolated tumor cells from predominant moderately-differentiated components. In five of the 10 node-positive primary lung adenocarcinomas, we additionally isolated peripheral well-differentiated components. To focus selectively on cancer cells, we applied laser capture microdissection (LCM). For comparison, we included six samples of macrodissected normal lung tissue.

Experiments and results

Firstly, we wished to identify the overall gene expression signature in all 42 samples by unsupervised hierarchical clustering with a set of highly variable genes. Two-way hierarchical clustering was performed using a Pearson correlation (Fig. 6). Eight of the 10 pairs of primary and metastatic tumors clustered next to each other. In these cases, the metastatic tumors had a higher similarity to their matching primary tumors than to all other tumors. In only two of the node-positive cases (cases 5 and 9), the metastatic tumors did

Springer

Fig. 5 Schematic design of this study. n + P, node-positive primary tumor; n-P, node-negative primary tumor; n + LN, node-positive lymph node; n + Pw, well-differentiated component of the node-positive primary tumor. Representative microscopic images of primary lung adenocarcinomas used in this study are shown, comprising moderately-differentiated components dominating large portions of the lesions and well-differentiated components evident in peripheral portions
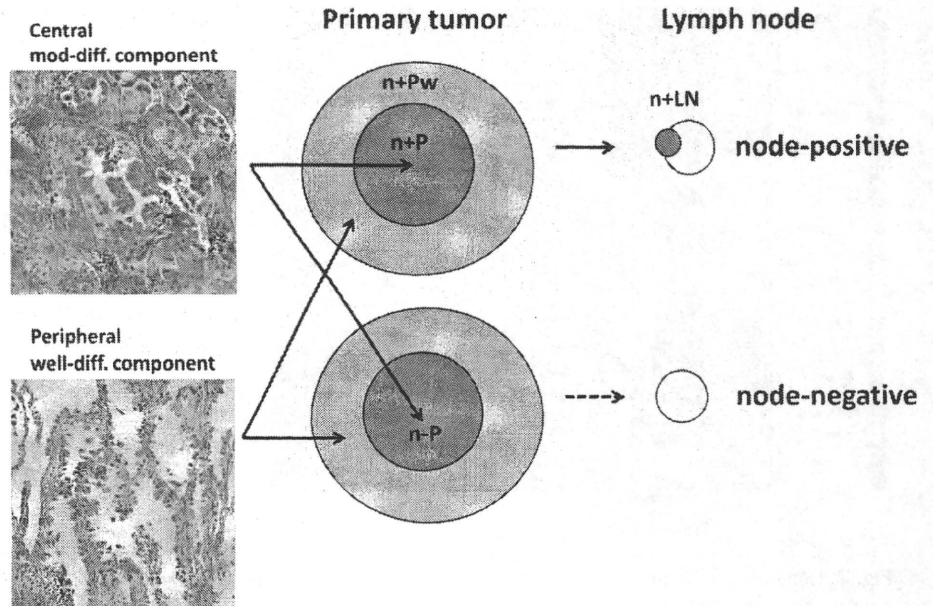
not cluster with their matching primary tumors, but a substantial similarity was still observed. In addition, all the peripheral well-differentiated components showed tight clustering with the predominant moderately-differentiated components from the same primary tumors. In the overall gene expression signatures, the central and the peripheral components from the same primary tumor were strikingly similar to each other.

To identify the gene expression signature of lymph node metastases, we performed a statistical comparison between the 10 pairs of primary and metastatic tumors using a paired *t*-statistic. Only 12 genes were yielded. For 11 of these genes, no significant differences were found between 10 lymph node metastases and 11 node-negative primary tumors, suggesting that they are not part of a metastatic expression signature. Only one gene, *Chromosome 4 open reading frame 7* (*C4orf7*) was significantly higher in the lymph node metastases than both node-positive and -negative primary tumors. However, as *C4orf7* is expressed characteristically by follicular dendritic cells found in lymph nodes, the high expression presumably resulted from contamination in the LCM process. It follows that no significant metastatic changes were detected between primary tumors and their lymph node metastases. The marked similarity between primary tumors and their lymph node metastases drove us to consider that the gene expression signature of lymph node metastasis might be acquired by the majority of primary tumor cells.

Next, to identify the metastatic expression signature detected in the primary tumors, we performed a statistical comparison (Welch's *t*-test) between 10 node-positive primary tumors and 11 node-negative primary tumors. This
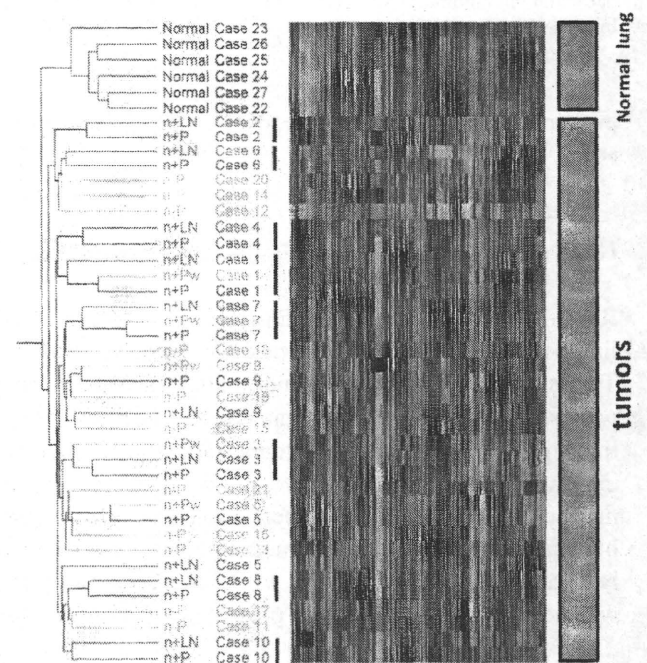
Fig. 6 Unsupervised hierarchical clustering for 2,451 genes against 42 samples comprising 10 pairs of node-positive primary tumors (n + P) and node-positive lymph nodes (n + LN), 11 node-negative primary tumors (n-P), 5 well-differentiated components of the node-positive primary tumors (n + Pw), and 6 normal tissues (Normal). Columns represent gene and rows represent samples. Note that eight of the 10 pairs of primary and metastatic tumors clustered next to each other (*bars*)

yielded 75 genes, comprising 37 with significantly higher expression in node-positive than node-negative primary tumors and 38 with significantly lower expression. The top discriminating gene was *homeobox B2* (*HOXB2*) with

higher expression in node-positive primary tumors. Malignant potential associated with ectopic *HOXB2* expression has been reported recently [21]. Down-regulated genes in node-positive primary tumors include *VAMP-associated protein A* (VAPA), involved in vesicle trafficking, and *Zinc finger protein 36 homolog* (ZFP36), which is also known as *tristetraprolin* (TTP) and is involved in degradation of tumor necrosis factor α. The *IQ motif containing GTPase activating protein 1* (IQGAP1), one of the molecular markers for lymph node metastasis identified by a microarray study using LCM [22], was also found to be included in the down-regulated genes.

The next issue was whether this 75-gene signature might be maintained throughout the metastatic process, and also be present in peripheral well-differentiated components of primary tumors. We therefore performed supervised hierarchical clustering of all the 42 samples against these 75 genes using a Pearson correlation (Fig. 7). Node-positive cases formed a distinct independent group, except one case (case 9), separate from node-negative tumors and normal lung tissues. The latter two clustered together. The node-positive group included the metastatic tumors and the primary well-differentiated components. Also in this metastatic gene expression signature, as with the overall gene

Fig. 7 Hierarchical clustering for the 75 genes against 42 samples comprising 10 pairs of node-positive primary tumors (n + P) and node-positive lymph nodes (n + LN), 11 node-negative primary tumors (n-P), 5 well-differentiated components of the node-positive primary tumors (n + Pw), and 6 normal tissues (Normal). Remarkably, nine of the 10 node-positive cases formed a distinct independent group. Pairs of primary and metastatic tumors clustered next to each other (*bars*)

expression signature, samples from the same case showed tight clustering. In leave-one-out cross-validation analysis, the 75 genes predicted their groups with 100% accuracy. Using real-time RT-PCR analysis, we validated our results for some of genes of interest from the 75-gene set.

Discussion

In this study, we could identify a 75-gene signature discriminating between node-positive and node-negative primary lung adenocarcinomas. Hierarchical clustering using this gene set generated a distinct independent group composed of node-positive cases, including the metastatic tumors and the peripheral well-differentiated components, separate from node-negative tumors and normal lung tissues. Striking transcriptional similarities were observed between samples from the same case and unsupervised hierarchical clustering showed tight clustering. Hierarchical clustering using the 75-gene set also showed tight clustering, reflecting similarity also in the metastatic gene expression signature. Indeed, statistical comparison of gene expression levels between pairs of primary tumors and their lymph node metastases revealed no differences responsible for the metastasis, implying that metastatic potential might be established early in the pathogenesis of tumors. This result is in keeping with recent array findings suggesting that metastatic potential is encoded in the bulk of a primary tumor [7]. More recently, D'Arrigo et al. [23] similalry showed striking transcriptional similarity using 10 pairs of matching primary colorectal cancers and distant metastases.

Several studies have resulted in lists of metastasis-related or malignancy-related genes in lung cancers [5–7, 22, 24]. However, most authors did not use microdissection but rather RNAs isolated from tumor masses. As their gene lists differed widely and had only few genes in common, the 75-gene list we identified also differed widely from theirs. Ein-Dor et al. [25] reported that thousands of samples are needed to generate a robust gene list for predicting outcome in cancer. Kikuchi et al. [22] used microdissected samples of 22 primary lung adenocarcinoma cases and identified 40 genes whose expression levels could separate cases according to their lymph node status. One of the 40 genes was *IQGAP1*, also included in our 75-gene metastatic signature. In our hospital, survival for p-Stage I lung cancer patients is good as compared with the literature. Whereas the reported 5-year survival for p-Stage I patients with non-small cell lung cancer is about 60% [1], it is 90% in our hospital [2]. We usually perform thorough dissection of lymph nodes and make a detailed histopathological examination. This accurate assessment of lymph node status is clearly advantageous for comparison of node-positive and node-negative tumors.
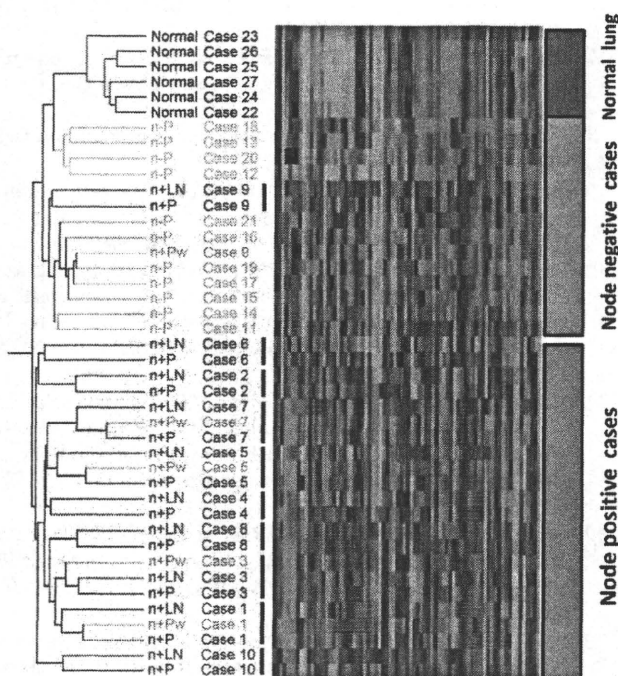
In the 75-gene set we identified, *HOXB2* was the top discriminating gene between node-positive and node–negative primary lung adenocarcinomas. Aberrant expression of *HOX* genes has been implicated in leukemias and various solid cancers, including lung cancers, with likely involvement of the gene products in features of malignant progression, such as invasion and metastasis. Overexpression of *HOXD3* is known to induce coordinate expression of metastasis-related genes in lung cancer cells [26]. A recent study further revealed ectopic *HOXB2* expression in pancreatic cancers and some proportion of precursor lesions, pancreatic intraepithelial neoplasias, possibly associated with a poor prognosis [21]. In our current study, we observed *HOXB2* overexpression not only in the central but also in the peripheral zones of node-positive primary tumors. Malignant potential associated with *HOXB2* expression might thus be acquired early in tumorigenesis.

Our results imply that the metastatic potential might be encoded in the entirety of each primary lung tumor including the morphologically less malignant component. This has profound clinical implications. It offers a rationale for therapeutic applications based on the expression profile of the primary tumor. Even if the peripheral component of the tumor is sampled by bronchoscopic or needle biopsy, the metastatic potential of the tumor could be predicted with accuracy. Such evaluation of metastatic potential would help spare unnecessary lymph node dissection for low-risk patients. However, the 75-gene signature needs to be confirmed using independent samples and further research is required to clarify the included molecular functions.

Very recently, using real time RT-PCR analysis, we investigated the transcriptional levels of the top metastasis-related genes using 96 independent test lung adenocarcinoma samples and investigated their correlations with prognosis [27]. We could document evidence that p-Stage I patients with HOXB2 up-regulation have a worse prognosis than those with HOXB2 down-regulation ($P = 0.0065$). Comparing tumors and corresponding normal lung tissue, we confirmed HOXB2 up-regulated lesions to have much higher HOXB2 expression than the corresponding normal tissue.

In conclusion

Recent studies support the hypothesis that metastatic potential is acquired early in tumorigenesis and that the majority of tumor cells have the potential to metastasize. Although gene expression profiles that can classify cancer patients according to the risk of recurrence have been found in many studies, most of these were retrospective. Very recently, by gene expression profiling, Potti et al. [9] proposed a "lung metagene model" that could identify individuals at increased risk for disease recurrence with

stage IA NSCLC. They are now planning to use this for a prospective randomized clinical trial. In the future, more emphasis needs to be placed on translational research to enable basic research findings to be applied in the clinic.

References

1. Brundage MD, Davies D, Mackillop WJ (2002) Prognostic factors in non-small cell lung cancer: a decade of progress. Chest 122(3):1037–1057. doi:10.1378/chest.122.3.1037
2. Miyoshi T, Satoh Y, Okumura S et al (2003) Early-stage lung adenocarcinomas with a micropapillary pattern, a distinct pathologic marker for a significantly poor prognosis. Am J Surg Pathol 27(1):101–109. doi:10.1097/00000478-200301000-00011
3. Inamura K, Shimoji T, Ninomiya H et al (2007) A metastatic signature in entire lung adenocarcinomas irrespective of morphological heterogeneity. Hum Pathol 38(5):702–709. doi:10.1016/j.humpath.2006.11.019
4. Garber ME, Troyanskaya OG, Schluens K et al (2001) Diversity of gene expression in adenocarcinoma of the lung. Proc Natl Acad Sci USA 98(24):13784–13789. doi:10.1073/pnas.241500798
5. Bhattacharjee A, Richards WG, Staunton J et al (2001) Classification of human lung carcinomas by mRNA expression profiling reveals distinct adenocarcinoma subclasses. Proc Natl Acad Sci USA 98(24):13790–13795. doi:10.1073/pnas.191502998
6. Beer DG, Kardia SL, Huang CC et al (2002) Gene-expression profiles predict survival of patients with lung adenocarcinoma. Nat Med 8(8):816–824
7. Ramaswamy S, Ross KN, Lander ES et al (2003) A molecular signature of metastasis in primary solid tumors. Nat Genet 33(1):49–54. doi:10.1038/ng1060
8. Liotta LA, Kohn EC (2003) Cancer's deadly signature. Nat Genet 33(1):10–11. doi:10.1038/ng0103-10
9. Potti A, Mukherjee S, Petersen R et al (2006) A genomic strategy to refine prognosis in early-stage non-small-cell lung cancer. N Engl J Med 355(6):570–580. doi:10.1056/NEJMoa060467
10. Sun Z, Aubry MC, Deschamps C et al (2006) Histologic grade is an independent prognostic factor for survival in non-small cell lung cancer: an analysis of 5018 hospital- and 712 population-based cases. J Thoracic Cardiovasc Surg 131(5):1014–1020. doi:10.1016/j.jtcvs.2005.12.057
11. Inamura K, Fujiwara T, Hoshida Y et al (2005) Two subclasses of lung squamous cell carcinoma with different gene expression profiles and prognosis identified by hierarchical clustering and non-negative matrix factorization. Oncogene 24(47):7105–7113. doi:10.1038/sj.onc.1208858
12. Brunet JP, Tamayo P, Golub TR et al (2004) Metagenes and molecular pattern discovery using matrix factorization. Proc Natl Acad Sci USA 101(12):4164–4169. doi:10.1073/pnas.0308531101
13. Travis WD, Brambilla E, Muller-Hermelink HK, Harris CC (2004) World health organization classification of tumours: pathology and genetics of tumours of the lung, pleural, thymus and heart. Springer, Berlin
14. Jones MH, Virtanen C, Honjoh D et al (2004) Two prognostically significant subtypes of high-grade lung neuroendocrine tumours independent of small-cell and large-cell neuroendocrine carcinomas identified by gene expression profiles. Lancet 363(9411):775–781. doi:10.1016/S0140-6736(04)15693-6
15. Virtanen C, Ishikawa Y, Honjoh D et al (2002) Integrated classification of lung tumors and cell lines by expression profiling.

Proc Natl Acad Sci USA 99(19):12357–12362. doi:10.1073/pnas.192240599

16. Sasatomi E, Finkelstein SD, Woods JD et al (2002) Comparison of accumulated allele loss between primary tumor and lymph node metastasis in stage II non-small cell lung carcinoma: implications for the timing of lymph node metastasis and prognostic value. Cancer Res 62(9):2681–2689

17. Kang Y, Siegel PM, Shu W et al (2003) A multigenic program mediating breast cancer metastasis to bone. Cancer Cell 3(6):537–549. doi:10.1016/S1535-6108(03)00132-6

18. Kakiuchi S, Daigo Y, Tsunoda T et al (2003) Genome-wide analysis of organ-preferential metastasis of human small cell lung cancer in mice. Mol Cancer Res 1(7):485–499

19. van 't Veer LJ, Dai H, van de Vijver MJ et al (2002) Gene expression profiling predicts clinical outcome of breast cancer. Nature 415(6871):530–536. doi:10.1038/415530a

20. Terasaki H, Niki T, Matsuno Y et al (2003) Lung adenocarcinoma with mixed bronchioloalveolar and invasive components: clinicopathological features, subclassification by extent of invasive foci, and immunohistochemical characterization. Am J Surg Pathol 27(7):937–951. doi:10.1097/00000478-200307000-00009

21. Segara D, Biankin AV, Kench JG et al (2005) Expression of HOXB2, a retinoic acid signaling target in pancreatic cancer and pancreatic intraepithelial neoplasia. Clin Cancer Res 11(9):3587–3596. doi:10.1158/1078-0432.CCR-04-1813

22. Kikuchi T, Daigo Y, Katagiri T et al (2003) Expression profiles of non-small cell lung cancers on cDNA microarrays: identification of genes for prediction of lymph-node metastasis and sensitivity to anti-cancer drugs. Oncogene 22(14):2192–2205. doi:10.1038/sj.onc.1206288

23. D'Arrigo A, Belluco C, Ambrosi A et al (2005) Metastatic transcriptional pattern revealed by gene expression profiling in primary colorectal carcinoma. Int J Cancer 115(2):256–262. doi:10.1002/ijc.20883

24. Xi L, Lyons-Weiler J, Coello MC et al (2005) Prediction of lymph node metastasis by analysis of gene expression profiles in primary lung adenocarcinomas. Clin Cancer Res 11(11):4128–4135. doi:10.1158/1078-0432.CCR-04-2525

25. Ein-Dor L, Zuk O, Domany E (2006) Thousands of samples are needed to generate a robust gene list for predicting outcome in cancer. Proc Natl Acad Sci USA 103(15):5923–5928. doi:10.1073/pnas.0601231103

26. Miyazaki YJ, Hamada J, Tada M et al (2002) HOXD3 enhances motility and invasiveness through the TGF-beta-dependent and -independent pathways in A549 cells. Oncogene 21(5):798–808. doi:10.1038/sj.onc.1205126

27. Inamura K, Togashi Y, Okui M et al (2007) HOXB2 as a novel prognostic indicator for stage I lung adenocarcinomas. J Thoracic Oncol 2(9):802–807. doi:10.1097/JTO.0b013e3181461987